Ana Rita Serra Pedro

Licenciatura em Farmácia

Genome editing to be applied in functional characterization of genetic variants in familial breast cancer patients

Dissertação para obtenção do Grau de Mestre em
Bioquímica para a Saúde

Orientador: Professora Susana Nunes da Silva, PhD

NOVA Medical School | Faculdade de Ciências Médicas da Universidade Nova de Lisboa

Fevereiro, 2021

Ana Rita Serra Pedro

Licenciatura em Farmácia

Genome editing to be applied in functional characterization of genetic variants in familial breast cancer patients

Dissertação para obtenção do Grau de Mestre em

Bioquímica para a Saúde

Orientador: Professora Susana Nunes da Silva, PhD

NOVA Medical School | Faculdade de Ciências Médicas da Universidade Nova de Lisboa

Júri:

Presidente: Professor Doutor António Sebastião Rodrigues;
Arguente: Doutor Pedro Rafael da Costa Antas;
Vogais: Professora Doutora Maria Teresa Nunes Mangas Catarino

NOVA Medical School | Faculdade de Ciências Médicas da Universidade Nova de Lisboa

Fevereiro, 2021

Agradecimentos

Finalizada esta etapa particularmente importante da minha vida, não poderia deixar de expressar o mais profundo agradecimento a todos aqueles que direta ou indiretamente me apoiaram nesta longa e atribulada caminhada e que contribuíram não só para a realização deste trabalho, como também para o meu crescimento pessoal.

Um agradecimento especial à minha orientadora, Doutora Susana Nunes da Silva por me ter recebido e permitido trabalhar neste projeto que lhe diz tanto, por todo o apoio e confiança que me foi dado ao longo deste ano e meio. Obrigada por ter sido mais do que uma "chefe" para mim e por ter acreditado nas minhas capacidades.

Ao Professor Sebastião Rodrigues, que sempre se disponibilizou para ajudar nos trabalhos. Obrigada pela partilha de conhecimentos e acima de tudo por ter sempre uma palavra de apoio e incentivo.

Ao Professor José Rueff, por me receber no Centro de Toxigenómica e Saúde Humana.

À Maria João Pires, ao Doutor Francisco Esteves e Doutor Bruno Gomes, pelo apoio e ajuda que me deram e por estarem sempre disponíveis para tal.

Às minhas companheiras de laboratório, sem as quais esta longa jornada não teria sido a mesma! Às meninas de nutrição por todas as conversas dos mais diversos temas e gargalhadas. À Daniela Dias, um agradecimento especial pelo apoio, as longas horas, as brincadeiras e acima de tudo por seres muito mais do que uma colega e espero que saibas o lugar especial que irás sempre ter. À Viviane Leite, a minha companheira de todas as horas, um obrigado especial por tornar os longos dias de laboratório mais leves e divertidos. Não tenho palavras de agradecimento que cheguem pelo papel tão importante que teve na minha vida, tanto profissional como pessoal. Por todo o apoio, alegria e dores partilhadas, obrigada.

Um agradecimento com muito carinho aos meus amigos e amigas, em particular à Cláudia Batista e Filipa Coutinho, que entraram na minha vida há muitos anos e que irão continuar outros tantos. Por todos os momentos de felicidade e loucura, pelos momentos sérios e de tristeza e principalmente pelo apoio incondicional, carinho e pela paciência que todos tiveram comigo.

Ao meu namorado, Carlos, que sempre me "aturou" com uma paciência enorme, sempre com um sorriso e uma palavra reconfortante. Obrigada pelo apoio e amor incondicional.

Por último, mas sem dúvida mais importante, à minha família que sempre me apoiou e acreditou em mim. Aos meus pais pelo apoio incondicional e por nunca me terem deixado desistir, é sem dúvida, graças a eles que estou aqui hoje. Ao meu irmão Miguel, mais do que um irmão, um amigo para os bons, maus e momentos assim-assim, sempre com uma piada seca pronta para me animar e um abraço.

A todos, um sincero obrigada por permitirem que esta seja uma realidade.

Abstract

Familial breast cancer (BC) is responsible for 15% of all BC cases being mainly linked to inherited variants in *BRCA* genes. Several genes associated with BC are mostly related to Homologous Recombination (HR), the main pathway to repair DNA double-strand breaks. The occurrence of genetic variants in these genes, such as *BRCA1* and *BRCA2,* might compromise the HR, thus the development of disease. In familial breast cancer the genetic counselling and the screening through genetic testing has been widespread increasing detection of variants of unknown significance (VUS). The biologic effect attributed to those VUS is mostly unclear, so functional assays need to be performed to characterize their mutational status.

In a previous study a VUS was identified in the *BRCA1* gene in healthy patients but with a relevant familial history of cancer. To study its functional relevance, we implemented an *in vitro* model using breast cell lines (MCF10-A and MCF-7). to introduce the VUS of interest with a genome editing tool, CRISPR-Cas9 and assess the cellular response through a genotoxic challenge with doxorubicin (DOX).

We successfully established MCF10-A heterozygous clone for the VUS. Several methodologies were selected to evaluate and compare the cellular response to genetic lesions: Comet, ɣ-H2AX and Annexin V assays. Also, we assessed the protein relative expression using Western Blot. The comet assay results showed a decreased sensitivity to DOX in MCF10-A VUS, yet, in ɣ-H2AX assay, we observed a higher % DSB. In Annexin V, MCF10-A VUS showed lower % of cells in necrosis. Lastly, the expression of BRCA1 protein was decreased in MCF10-A VUS.

Overall, the results show a decreased susceptibility to DOX for the VUS cell line, suggesting a benign behaviour. Nonetheless more functional assays need to be performed to understand their role on cancer risk.

Keywords: *BRCA1;* CRISPR-Cas9; Familial Breast Cancer; MCF10-A; MCF-7; Variants of Unknown Significance (VUS).

Resumo

O cancro da mama (CM) familiar representa 15% de todos os casos de CM, estando principalmente relacionado a variantes hereditárias nos genes *BRCA*. Vários genes ligados ao CM estão sobretudo relacionados com a Recombinação Homóloga (RH), a principal via de reparação de quebras de cadeia-dupla de DNA. A presença de variantes genéticas nestes genes, como o *BRCA1* e *BRCA2*, pode comprometer a RH e consequentemente o desenvolvimento da doença. No cancro da mama familiar, o aconselhamento genético e a triagem através de testes genéticos têm se tornado padrão, aumentando a deteção de variantes de significado desconhecido (VUS). O efeito biológico atribuído às VUS é pouco claro, sendo necessários ensaios funcionais para caracterizar o seu significado clínico.

Num estudo anterior, uma VUS foi identificada no gene *BRCA1* em pacientes saudáveis, mas com histórico familiar de cancro relevante. Para estudar a sua relevância funcional, implementamos um modelo *in vitro* com linhas celulares de mama (MCF10-A e MCF-7) para introduzir a VUS de interesse com uma ferramenta de edição genómica, CRISPR-Cas9 e avaliar a resposta celular através de um desafio genotóxico com doxorrubicina (DOX).

Introduzimos com sucesso a VUS como clone heterozigoto nas MCF10-A. Várias metodologias foram selecionadas para avaliar e comparar a resposta celular às lesões genéticas: ensaios do Cometa, ɣ-H2AX e Anexina V. Adicionalmente, avaliamos a expressão relativa da proteína através de Western Blot. Os resultados do ensaio do cometa mostram uma diminuição da sensibilidade à DOX no MCF10-A VUS, porém, no ensaio ɣ-H2AX, observamos um maior % de quebras e cadeia-dupla. Na Anexina V, o MCF10-A VUS apresentou menor % de células em necrose. Por último, a expressão da proteína BRCA1 encontra-se diminuída nas MCF10-A VUS.

No geral, os resultados mostram uma diminuição da suscetibilidade à DOX para a linha celular com a VUS, sugerindo um efeito benigno. No entanto, são necessários mais ensaios funcionais para entender o seu papel no risco de cancro.

Palavras-chave: *BRCA1;* Cancro da mama familiar; CRISPR-Cas9; MCF10-A; MCF-7; Variante de significado desconhecido (VUS).

Abbreviations

ATM - Ataxia telangiectasia syndrome;

ATR - ATM and rad3-related;

BC – Breast Cancer;

BER - Base-excision repair;

BRCA1 – Breast Cancer gene 1;

BRCA2 – Breast Cancer gene 2;

BRIP1 - BRCA1 Interacting Protein C-Terminal Helicase 1;

Cas - CRISPR-associated proteins;

CDH1 - Cadherin 1;

CHEK2 - Checkpoint kinase 2;

CPT – Camptotecin;

CRISPR - Clustered regularly interspersed short palindromic repeats;

DDR- DNA damage response;

DMEM - Dulbecco's Modified Eagle Medium;

DOX – Doxorubicin;

DSB - Double strand breaks;

DSBR - Double-strand break repair;

FBS – Fetal Bovine Serum;

GI - Genomic instability;

H_2O_2 - Hydrogen peroxide;

HR - Homologous recombination;

IR - Ionizing radiation;

LOH – loss of heterozygosity;

MMEJ - Microhomology mediated end-joining;

MMR - Mismatch repair;

MRE11 - Meiotic Recombination 11 homolog;

MRN - MRE11, RAD50 and NBS1;

NBS1 - Nijmegen Breakage Syndrome 1;

NER - Nucleotide-excision repair;

NGS - Next Generation Sequencing;

NHEJ - Non-homologous end-joining;

PALB2 - Partner and Localizer of *BRCA2*;

PAM - Protospacer adjacent motif;

PARPi - Poly-ADP-ribose polymerase inhibitors;

PTEN - Phosphate and tensin homolog deleted on chromosome ten;

RAD50 - DNA repair protein RAD50;

RAD51 - DNA repair protein RAD51;

RING - Really interesting new gene;

ROS - Reactive oxygen species;

SCGE - single-cell gel electrophoresis;

sgRNA - single guide RNA;

SSA - Single-strand annealing;

SSBR - Single-strand break repair;

ssODNs - single-stranded DNA oligonucleotides;

STK11 - Serine/Threonine Kinase 11;

TP53 - Tumor protein 53;

UV - Ultraviolet light;

VUS - Variants of unknown significance.

List of Contents

List of Figures

List of Tables

1. Introduction

Introduction

1.1. Breast Cancer

Cancer is a designation for a large group of diseases. It is characterised by an unregulated growth and proliferation of cells with the ability to metastasise into different organs through the blood and lymphatic systems (World Health Organization, [s.d.]). As cancer incidence and mortality has quickly increased worldwide, it has become one of the most important barrier to increase life expectancy in the 21st century (Bray *et al.*, 2018).

Breast cancer (BC) is the most common cancer, and one of the leading causes of cancer-related deaths. In 2020, it was estimated that 2.26 million women were diagnosed with BC and 684 thousand died from this disease – corresponding to almost 16% of all cancer deaths. In case of Portugal, 7 thousand of new cases of female BC were estimated in 2020, about 26% of all cancer's incidence (GLOBOCAN 2020, [s.d.]).

BC patients have a higher survival rate when compared with other types of cancer, most likely due to the breast not being a vital organ. In addition, mastectomy and chemotherapy are improving patient's survival. Even so, this disease has repercussions besides the physical sequelae of the treatment or surgery, such as mental and emotional unbalance. Not only due to chemotherapy, but also the uncertainty of relapses, metastasis, or even death itself. With this in mind, much more can be done; for instance, more personalised treatments and monitoring, but also clinical management of patients at high-risk with prevention and screening, and a better understanding of the underlying tumour biology (Feng *et al.*, 2018).

Ageing and growth of the population are the major risk factors for BC. Furthermore, its development is associated with being a woman, race, ethnicity, lifestyle, hormonal and environmental factors (Bray *et al.*, 2018; Harbeck *et al.*, 2019). Beyond all of these, one significant risk is genetic predisposition. It is described that the risk of developing BC increases two-fold if the patient has a first-degree relative, such as a mother, a sister, or a daughter who were diagnosed with BC (Feng *et al.*, 2018).

Sporadic cancer is responsible for 70 to 80% of all BC cases, it occurs by chance and typically in advanced ages. Hereditary breast cancer is prevalent in 5 to 10% of all BC cases, and it is mostly due to germinal mutations in specific genes, such as high penetrance genes - *BRCA1* and *BRCA2* - that increase the susceptibility to develop cancer. Moreover, this susceptibility is transmitted to the family members with an

evident hereditary pattern. Last, but not least, close to 15% of all cases are familial breast cancer, being linked not only to high penetrance genes but also, other shared factors, like environment or lifestyle. In contrast with the hereditary cases, it is not possible to identify a clear pattern of inheritance in these cases (Augusto *et al.*, 2018). Statistically, women bearing a mutation in *BRCA1* have a 55 to 65% lifetime risk of developing BC, whereas women with a mutation in *BRCA2* have a 45% risk (Feng *et al.*, 2018).

The exact mechanism by which BC is initiated is unknown; BC is a highly heterogenous disease, between and within tumours. Due to this fact, much effort has been made to molecularly characterize BC and delineate its formation and progression (Harbeck et al., 2019). This heterogeneity is promoted by genomic instability (GI), a characteristic of most solid cancer and a key hallmark of cancer (Hanahan e Weinberg, 2011; Kalimutho *et al.*, 2019). GI arises, not only due to defects in the DNA damage repair and response, but also promotes a higher vulnerability towards DNA damaging agents thus increased replication stress (Amir *et al.*, 2010; Hoeijmakers, 2009; Prakash *et al.*, 2015).

1.2. DNA Damage Repair and Response

Cells have an important role for the perpetuation of life not only to keep us alive, but also and foremost, to perpetuate life by preserving our genomic information. The basic unit of inheritance – DNA - is an intrinsically reactive molecule and highly susceptible to chemical modifications (Chatterjee e Walker, 2017). Remarkably, each of the ~10^{13} cells in the human body undergoes tens of thousands of DNA lesions every day (Jackson e Bartek, 2009), due to constant exposure to numerous damaging agents. These can be exogenous - like environmental stresses, such as ultraviolet light (UV), ionizing radiation (IR), chemicals, toxins and pollutants – or endogenous, which results from regular cellular metabolism - such as DNA methylation, replication errors, alkylation, hydrolysis and reactive oxygen species (ROS) (Chatterjee e Walker, 2017; Hoeijmakers, 2009). Both types can induce DNA lesions, which if left unrepaired or repaired inaccurately, can compromise the genome integrity (Figure 1.1).

Therefore, cells have evolved a complex series of interlinked mechanisms to detect, signal and repair the DNA damage, designated the DNA-damage response (DDR) (Chatterjee e Walker, 2017; Jackson e Bartek, 2009). Cells can induce arrest of cell-cycle progression at specific checkpoints in G1, S, G2 and M to allow the repair of lesions before they become permanent. In addition, if the lesion is left unrepaired or is too significant it can be detected by inhibition of both transcription, replication, and

chromosome segregation, thus leading to apoptosis. This consequence limits the passage of mutations of the progeny cells, along with the prevention of diseases, such as cancer or inborn diseases (Hoeijmakers, 2001).

Cells have five main DNA repair pathways: Base-excision repair (BER), Nucleotide-excision repair (NER), Mismatch repair (MMR), single-strand break repair (SSBR) and double-strand break repair (DSBR). This last one has two major repair pathways, homologous recombination (HR) and non-homologous end-joining (NHEJ), but also, not so frequent, called single-strand annealing (SSA) and microhomology mediated end-joining (MMEJ) (Figure 1.2). Each has various signalling proteins and are drawn by different types of damage at the site (Amir *et al.*, 2010; Hoeijmakers, 2001).

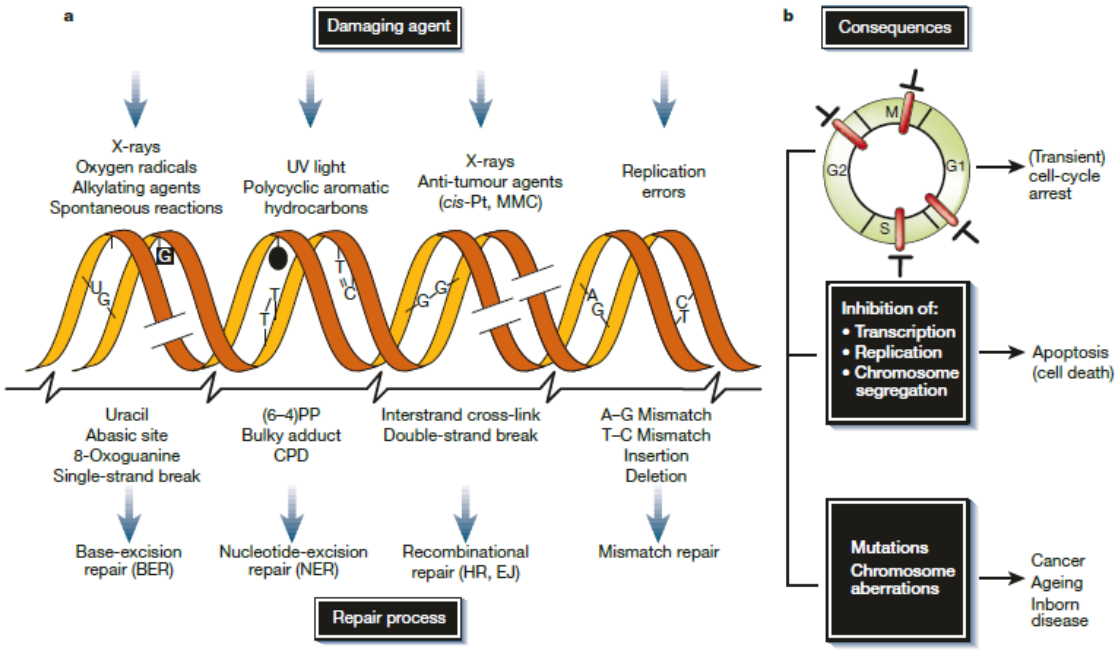

Figure 1.1 - DNA damage repair pathways and consequences. a. DNA damaging agents lead to specific DNA lesions that are repaired through one of the five most common repair processes (Base-excision repair - BER, Nucleotide-excision repair - NER, Homologous recombination - HR, Non-homologous end-joining - NHEJ or Mismatch repair - MMR). **b.** DNA damage can induce arrest of cell-cycle progression, inhibition of both transcription and replication, and chromosome segregation, which leads to apoptosis. It can also introduce genomic instability, such as mutations or chromosome aberrations, this being the main causes of cancer, ageing or even inborn diseases (Hoeijmakers, 2001).

Due to GI, tumour cells have a higher capability of adaptability and survival (Kalimutho *et al.*, 2019). Moreover, they frequently usurp the DDR pathways to generate double strand breaks (DSB) and enhance mis-repair (Aparicio, Baer e Gautier, 2014; Shibata e Jeggo, 2014). DSB are extremely hazardous lesions that may lead to genomic rearrangements such as aneuploidy and genetic aberrations or even cell death. DSBs occur when both strands of the DNA duplex are broken, often due to

exposure to exogenous agents, such as IR. Furthermore, during normal cell metabolism the production of ROS, which oxidize the bases, can trigger both single and double strand breaks. Also, as DNA replication forks face unrestored DNA lesions, this may lead to a fork collapse (Amir *et al.*, 2010; Aparicio, Baer e Gautier, 2014; Bolderson *et al.*, 2009; Chapman, Taylor e Boulton, 2012).

There are two major pathways of DSB repair - NHEJ and HR – based on whether sequence homology is used to join the DSB ends (Figure 1.3) (Aparicio, Baer e Gautier, 2014). NHEJ does not require sequence homology being active through the whole cell cycle, mainly during G1 phase. On the contrary HR, requires a sister chromatid present to copy and restore the DNA damaged, so during S an G2 phases it prevails over NHEJ.

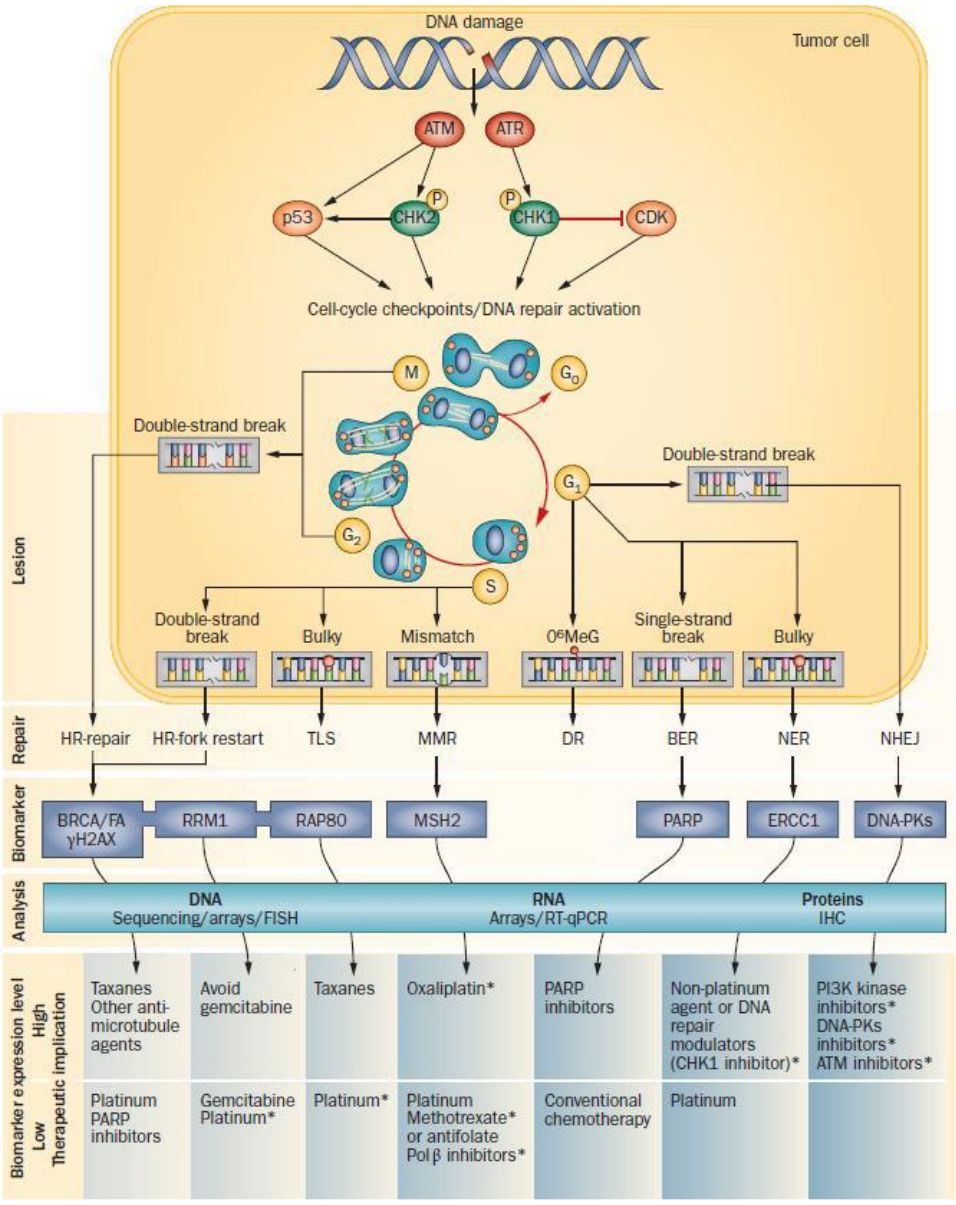

Figure 1.2 - DNA damage and its main repair pathways with key proteins/biomarkers involved. Adapted from (Postel-Vinay et al., 2012).

This is not the only difference between these repair pathways. HR is error-free, conservative and dependent on *BRCA1* and *BRCA2*, with a key protein (RAD51) (Lord e Ashworth, 2016; Prakash *et al.*, 2015). In contrast and as an alternative, NHEJ is error-prone (introduces deletions or insertion - INDELS), non-conservative since it does not use a sister chromatid, it simply re-ligates the DSB, which increases the number of deletions, translocations and chromosomal instability (Aparicio, Baer e Gautier, 2014; Chapman, Taylor e Boulton, 2012).

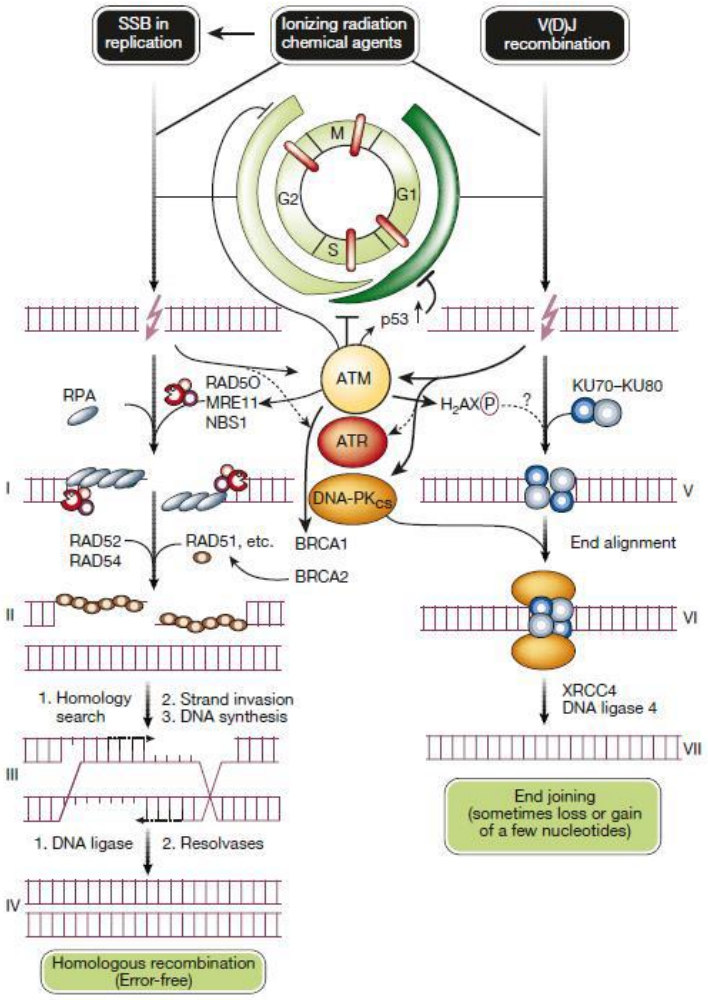

Figure 1.3 - The homologous recombination (HR) and non-homologous end-joining (NHEJ) pathways (Hoeijmakers, 2001).

Nevertheless, although NHEJ and HR are the main pathways for the repair of DSBs, there are others alternatives less used by the cells, SSA and MMEJ. SSA occurs when HR is compromised, as in *BRCA1/2* deficient cells; it anneals regions with a similar sequence on either side of the DSB, which leads to a deletion of the interceding sequence, or a translocation whether it is paired to a sequence on a distinct chromosome. While SSA repair can be initiated by homologous sequences of various lengths, MMEJ only needs a few nucleotides to be active. This last pathway is active

throughout the cell cycle, same as NHEJ. However, the inappropriate use of annealing-mediated DSB repair can result in the formation of pathological chromosomal translocations (Aparicio, Baer e Gautier, 2014).

Unsurprisingly, the appropriate DSB repair pathway has a crucial impact on genomic integrity: defects in high-fidelity DNA damage repair machineries, like HR, can increase GI and lead to a greater reliance on compensatory, and often error-prone, DNA damage response and survival pathways, thus cancer (Prakash *et al.*, 2015).

1.3. Genetic of Breast Cancer: The role of *BRCA* genes

Several genes which are associated with BC are, as expected, related to pathways of the DDR. Different susceptibility genes may have varying degrees of penetrance; thus, some genes have a higher relative risk of causing a specific type of cancer than others (Economopoulou, Dimitriadis e Psyrri, 2015). These can be divided into three categories based on their penetrance: high penetrance genes (*BRCA1, BRCA2, PTEN, TP53, CDH1,* and *STK11*), moderate penetrance genes (*PALB2, ATM, BRIP1,* and *CHEK2*) and low penetrance genes (Rousset-Jablonski e Gompel, 2017; Shiovitz e Korde, 2015). Most of BC cases result from germline pathogenic mutations in *BRCA1* and *BRCA2* (Shiovitz e Korde, 2015).

BRCA genes play a wide array of cellular functions essential for genomic stability, not only at DNA damage response and cell cycle checkpoints, but also modulation of gene transcription, cell cycle progression and therapy resistance. As tumour suppressors, when mutated these genes contribute to the development of different types of cancer; for instance, they are associated to approximately 20% of familial breast and ovarian cancers (Gorodetska, Kozeretska e Dubrovska, 2019; Lord e Ashworth, 2016; Sharma *et al.*, 2018). Hence, the chances of having BC are highly increased in families or certain groups with *BRCA* mutations, like Ashkenazi who bear a highly specific and restricted mutation in these genes (Feng *et al.*, 2018; Rousset-Jablonski e Gompel, 2017; Winters *et al.*, 2017).

Furthermore, common genetic alterations are associated with heterozygous *BRCA1* or *BRCA2* mutations, and these include loss of the wild-type *BRCA1* or *BRCA2* allele (LOH). In the absence of LOH, haploinsufficiency of *BRCA* activity may cause enough GI to promote tumorigenesis (Pathania *et al.*, 2014; Roy, Chun e Powell, 2012). Although some data suggest that loss of the wild-type allele is not be required for tumorigenesis, most BC cases present LOH (Roy, Chun e Powell, 2012).

1.3.1. BRCA1 gene

BRCA1 gene is located on chromosome 17q21.3 and encodes 1863 amino acids. It consists of a multidomain protein with 24 exons, essential for multiple functions (Gorodetska, Kozeretska e Dubrovska, 2019; Shiovitz e Korde, 2015). Its protein is divided into four main domains: a highly conserved zinc-binding RING (really interesting new gene) finger domain located close to the N-terminus, two BRCT (BRCA1 C-terminal) domains at the C-terminus, NLS (nuclear localization signals) and one coiled coil domain at the central domain (Figure 1.4.a). BRCT is vital for repairing DSBs through HR, depending on which protein it interacts with, BRCT gives rise to four complexes A, B, C and D. Each one of them is key for HR at different stages. ɣ-H2AX signals the chromatin surrounding the DSB so that the BRCA1-A complex gets recruited and adverts the resection of the DNA. Both BRCA1-B and -C are critical for DNA end resection, which leads to single-stranded DNA (ssDNA) ends formation. BRCA1-C complex consists of CtIP and MRN (Mre/RAD50/Nbs1) and this complex association is cell cycle dependent, occurring in late S and G2 phases. Moreover, it enhances the nuclease activity of MRN, promoting DSB resection, facilitating DNA repair via HR over NHEJ. However, dissociation of the complex in G2/M checkpoint control, promotes apoptosis in damaged cells. Lastly, BRCA1-D complex recruits PALB2, BRCA2 and RAD51 to the DSB. The two latter proteins stimulate strand invasion (Christou e Kyriacou, 2012; Gorodetska, Kozeretska e Dubrovska, 2019; Roy, Chun e Powell, 2012; Sharma *et al.*, 2018).

Also, BRCA1 protein undergoes hyperphosphorylation when in presence of DSB. This protein is phosphorylated mainly by the DNA damage sensors - ataxia telangiectasia syndrome (ATM), ATM and rad3-related (ATR), and checkpoint 2 (Chk2). Interestingly, DNA checkpoint-associated kinases have been shown to phosphorylate specific residues of BRCA1, activating the protein to participate in different multiprotein complexes and in different signalling pathways, such as S-phase and G2-M checkpoint activation, and regulation of apoptosis through caspase-3 activation. Some genetic polymorphisms were found to affect numerous phosphorylation sites in the BRCA1, by eliminating kinase binding - essential for DSB repair through HR (Ouchi, 2006; Tram, Savas e Ozcelik, 2013; Yarden, 2006).

Most of the mutations found in this gene are frameshift or nonsense mutations, which result in truncated proteins. Only 2% of missense mutations in *BRCA1* are pathogenic, still it is difficult to discriminate them from polymorphisms (Sharma *et al.*, 2018).

1.3.2. BRCA2 gene

BRCA2 is located on chromosome 13q12.3, which encodes a large 3418 amino acids protein (Figure 1.4.b). More than 1800 genetic variants have been identified in this gene, the most frequent ones are frameshifts, deletions and nonsense variants and result in premature truncation or non-functional protein. There are also some missense mutations, although their pathogenicity is hard to validate. Just like *BRCA1, BRCA2* also is involved in the repair of DSBs through HR. RAD51 recruits BRCA2, forming a complex which is recruited to the DSB. Moreover, it possesses a DNA-binding domain that binds ssDNA to double-stranded DNA (dsDNA), which is most likely implicated in the formation of the RAD51 filament and accelerated accelerate replication protein A (RPA) - displacement (Roy et al., 2012).

Identically, *BRCA2* has some polymorphic variants that can alter the phosphorylated sites, altering the kinases specificities and biological role, such as ATM and CDK2. These are involved in DNA repair, cell cycle regulation, transcription or response to DNA damage, like HR (Tram, Savas e Ozcelik, 2013).

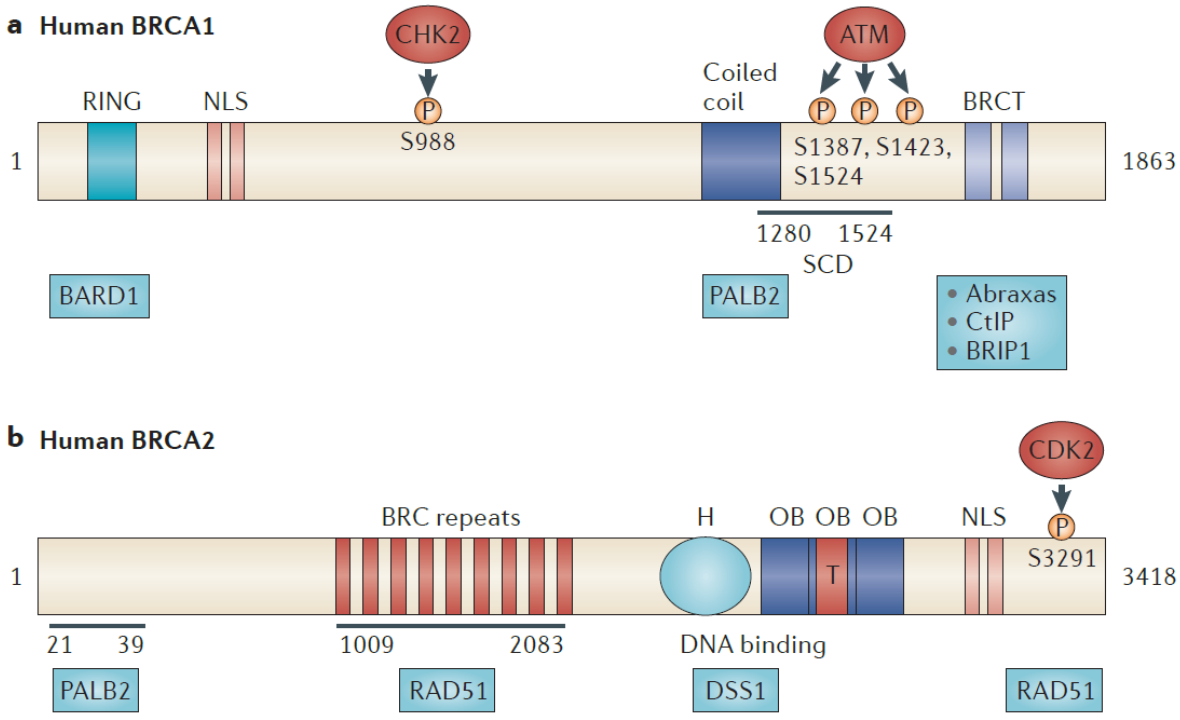

Figure 1.4 - BRCA1 and BRCA2 functional domains. (Adapted from Roy, Chun e Powell, 2012)

1.4. Variants of Unknown Significance

With the increasing public awareness of breast cancer hereditary syndromes, many women consider genetic testing for themselves and their close relatives, in particular when multiple relatives have cancer pointing out to a familial component. Genetic testing for *BRCA* genes along with other susceptibility genes have become a standard, thanks to advances in Next Generation Sequencing (NGS) which allows simultaneous testing for mutations in multigene panels (Lerner-Ellis *et al.*, 2015; Ma *et al.*, 2018). Nevertheless, these gene panels have become a burden for clinicians and genetic counsellors since they lead to an increase in the detection of variants in high or moderate penetrance genes without established clinical guidelines - variants of unknown significance (VUS). VUS is a variation in a genetic sequence for which the association with disease risk is still unclear. Due to insufficient epidemiological evidence and rarity of finding, VUS are difficult to classify as pathogenic or benign. For instance, carriers of VUS and their family members cannot take advantage of the risk assessment, prevention, and therapeutic measures that are available to carriers of known deleterious mutations. These ambiguous outcomes raise the pressing need to a better assessment of the risk associated to establish clinical guidelines, not only for the clinicians, but most importantly for the patients carrying these kinds of variants. Furthermore, around 39% of VUS carriers are counselled to undergo prophylactic surgery without knowing the relevance of the variant in developing cancer. (Chern *et al.*, 2019; Millot *et al.*, 2012; Santos *et al.*, 2014; Shirts, Pritchard e Walsh, 2016; Welsh *et al.*, 2017; Yoon *et al.*, 2017).

There are around 1500 different known VUS in *BRCA1* and *BRCA2* genes, many of which with the need of reclassification (Millot *et al.*, 2012; Welsh *et al.*, 2017). The majority of these variants are in-frame INDELs, missense or silent variants, whose effect on the protein structure cannot be directly inferred, exonic and intronic shifts, that may affect pre-mRNA splicing, and also regulatory sites (Augusto *et al.*, 2018; Radice *et al.*, 2011). The pathogenicity or predisposition to a certain disease or cancer, are generally associated to variants that introduce premature stop codons, or affect mRNA integrity and/or stability, giving rise to functionally compromised proteins (i.e. truncation), whereas a change in an amino acid residue caused by a VUS is conserved in the corresponding protein. Thus, a VUS may not lead to premature termination of a protein, hampering its classification. Moreover, it is still not clear whether such subtle changes can alter the function of the protein sufficiently to predispose to cancer (Radice *et al.*, 2011).

Another key point is whether the variant is in a functional domain of the protein. For example, if the VUS is within the RING-finger domain of the BRCA1, this is most likely to result in functional loss. However, if the variant is identified in the exon-intron boundaries, its effect is more difficult to assess, due to the involvement in the splicing process. Variants identified in well conserved functional domains are considered deleterious, such as variants for which the available evidence indicates the likelihood, but not definite proof, that the mutation is deleterious, hence further supporting steps are needed in the study of VUS (Calò *et al.*, 2010).

Currently, there are several strategies for the analysis of VUS; these include multifactorial prediction models (based on case-control studies, family history of cancer, co-segregation, co-occurrence, and loss of heterozygosity), *in vitro* assays, and *in silico* prediction tools. The most often use are *in silico* prediction tools, which provide vital information on the theoretical effect of the VUS on protein structure and splicing mechanisms; nevertheless, their impact on protein function cannot be directly inferred from sequence information, precluding assessment of their pathogenicity. Therefore, an essential but still not clarified question is the possible role of these gene variants and their potential effect on cancer risk, which only functional assays can answer (Calò *et al.*, 2010; Millot *et al.*, 2012).

The identification and characterization of genetic variant associations with clinical phenotypes is an ambitious goal in medical research, and the development of *in vitro* study models has been extremely important in pharmacogenomics, especially in drug discovery and drug response.

1.5. CRISPR-Cas 9

Genome editing holds enormous potential for applications across basic science, medicine and biotechnology. Several approaches have been developed, to improve the extent and effectiveness of gene editing, many of which in eukaryotic cells and animal models of human disease. One approach in specific, known as CRISPR, short for clustered regularly interspersed short palindromic repeats and its CRISPR-associated proteins (Cas), has generated a lot of excitement in the scientific community. CRISPR-Cas systems were discovered in *E. coli* as a bacterial adaptive immune system against foreign viral DNA (Ran *et al.*, 2013). By the time of its discovery, there were already some genome tools based on nuclease activity, like TALENs or zinc fingers, nevertheless, CRISPR technique stands out by being faster, cheaper, more accurate, more specific, more efficient and flexible enhancing its application in different targets from cell types to full organism. Briefly, the mechanism around this

approach starts with (Figure 1.5) the design of a small RNA molecule called single guide RNA (sgRNA), which guides the Cas9 nuclease to a specific target sequence of DNA to generate a DSB, ascertained by a 20 nucleotide sequence that heralds three base pairs upstream of a protospacer adjacent motif (PAM) sequence, which can either be NGG or NAG. Next, the DSB can be repaired by one of two mechanisms – HR or NHEJ. HR is more conservative, due to the use of DNA template for a more precise modification. On the contrary, NHEJ is error-prone, as it frequently leads to insertion of INDELs at the cut site causing obstruction of the coding sequence (Zhan *et al.*, 2019). Also, CRISPR-Cas9 can introduce the repair template using single-stranded DNA oligonucleotides (ssODNs), which supply a productive and effortless procedure for assembling modifications to the genome, such as single-nucleotide mutations to functionally analyse genetic variations (Ran *et al.*, 2013; Zhan *et al.*, 2019). Besides, the efficacy of genome editing with Cas9 makes it possible to change multiple targets simultaneously, allowing for more unbiased genome-wide functional screens to identify genes that play an essential role in a phenotype of interest (Zhang, Wen e Guo, 2014).

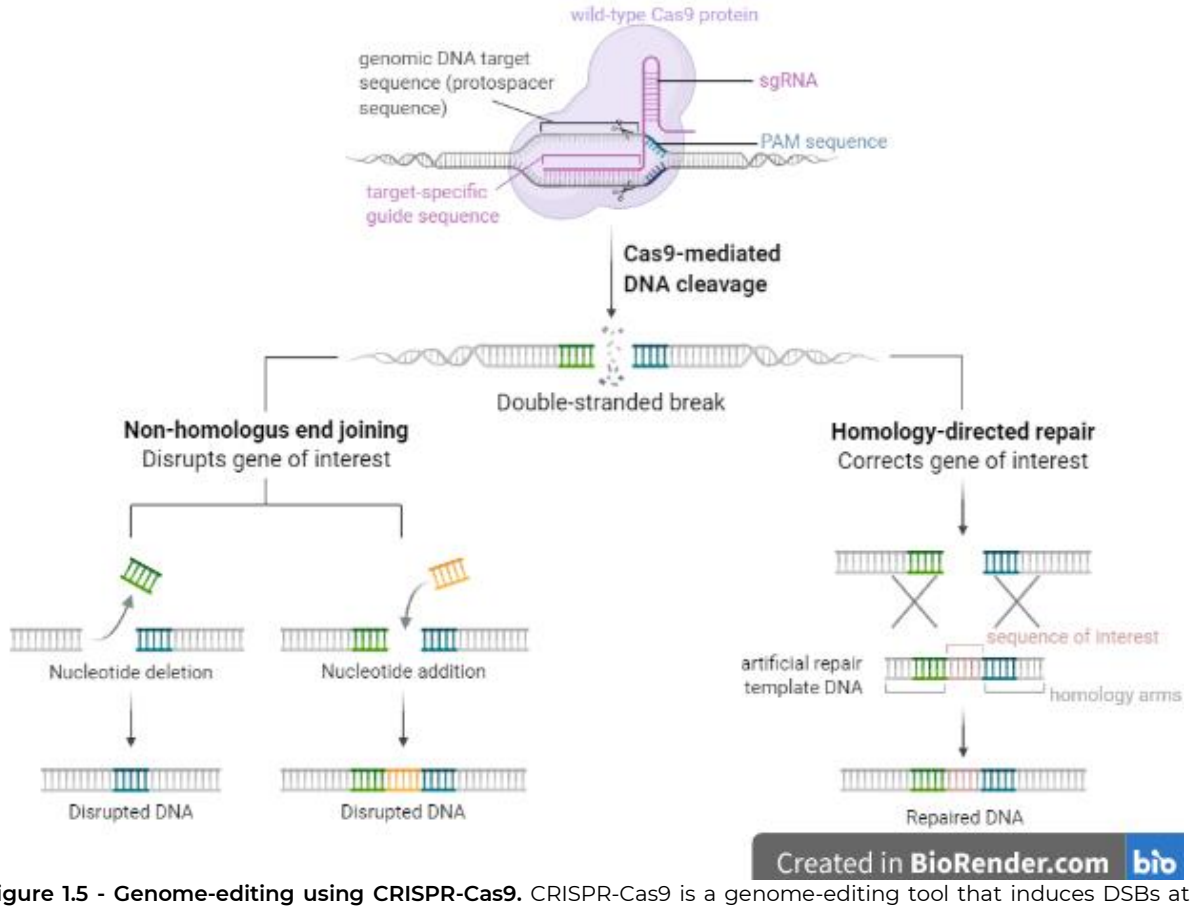

Figure 1.5 - Genome-editing using CRISPR-Cas9. CRISPR-Cas9 is a genome-editing tool that induces DSBs at specific target DNA sites by the combined action of a sgRNA, that recognizes a particular DNA sequence, and the Cas9 nuclease around the PAM sequence. Random indels or precise modifications are introduced into the genomic DNA by the NHEJ or HR pathway. Created with Biorender.

1.6. Functional assays

As stated before, functional assays are essential to better understand the role of gene variants on cancer risk. Hereupon, these are systematics experiments that are designed to determine the involvement of a protein in a particular cellular pathway or biological process. So, we can infer, directly or indirectly, the impact of gene variations on protein function by combining available genetic and epidemiological data (Millot *et al.*, 2012). By imposing a genotoxic challenge, there is an induction of DNA breaks, which can either be ssDNA or dsDNA breaks so that one can determine the impact of these lesions on genes related to such break's repair.

1.6.1. Doxorubicin

Doxorubicin (DOX) belongs to the anthracycline group of chemotherapeutic agents. Even though DOX is inherently toxic to non-cancerous cells, in its unaltered form, it is still one of the most used drugs in cancer treatment. This nonselective frontline drug is internalised via passive diffusion, and binds to its target enzymes, topoisomerase I and II, thus building several cytotoxic effects, such as covalent cleavage complexes, which will lead to apoptosis.

Figure 1.6 depicts a simplistic representation of the mechanism of action of DOX. This drug can intercalate the DNA by itself, causing breakage of DNA strands and constraining both DNA and RNA polymerases synthesis. Consequently, there is halting of DNA replication as well as RNA transcription. Also, there is a production of free radicals, like ROS, which will then boost DNA lesions, and inevitably cell death. (Johnson-Arbor e Dubey, 2020; Meredith e Dass, 2016).

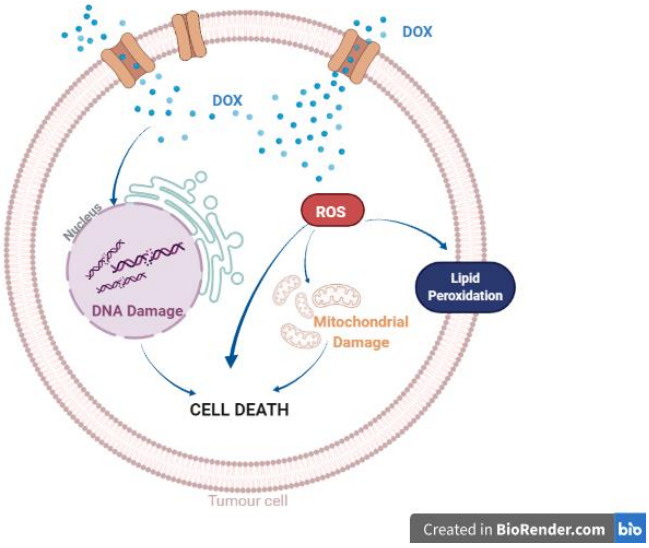

Figure 1.6 – Mechanism of action of Doxorubicin (DOX). DOX is a chemotherapeutic agent which leads tumour cells to their death through induction of multiple cell damages. For instance, DNA damage, production of reactive oxygen species (ROS), and membrane damage with lipid peroxidation. Created with BioRender.com.

1.7. Hypothesis and goals

Working hypothesis

Several *in silico* tools provide vital information on the theoretical effect of the VUS on protein structure and splicing mechanisms; nevertheless, their impact on protein function cannot be directly inferred from sequence information, precluding assessment of their pathogenicity. Therefore, the role of these variants and the role they play on cancer risk is still unclear.

In previous studies a VUS was identified in the *BRCA1* gene in patients with no cancer but showing a relevant familial history of cancer. Thus, by taking advantage of these previous results of such patients, we intended to create a biological model to characterise *in vitro* the functions of the VUS identified in *BRCA1*.

Main Goal

As stated before, thanks to a previous study it was possible to identify one VUS in the *BRCA1* gene. In order to study its functional relevance, our main goal is to implement an *in vitro* model using breast cell lines (MCF10-A and MCF-7) to introduce the VUS of interest with a genome editing tool, CRISPR-Cas9. MCF10-A is a non-tumorigenic cell-line, being the best line for a clearer insight if the VUS is benign or pathogenic. On the other hand, MCF-7 is a breast cancer cell-line, poorly aggressive and non-invasive, therefore the variant can be a potential enhancer of tumour aggressiveness. After establishing this approach, we intended to assess the functional relevance of the VUS under study after a genotoxic challenge.

One improvement of this method relies not only in no limitation to sample size allowing an efficient follow-up but also the opportunity to replicate studies and extend it to study other VUS. Furthermore, optimizing the genome editing methodologies will be useful to answer pertinent questions related to haploinsufficiency identified and how it can modulate the cellular response to cancer development.

2. Materials and Methods

2.1. Variant of Unknow Significance Identification

In a previous study by Adubeiro, R., several family's individuals, two with no genetic alterations and no disease, two BC patients (mother and daughter), both with a pathogenic mutation in the *ATM* gene, and lastly, two healthy individuals with high occurrence of cancer in the family (Figure 2.1.), were screened by NGS for eleven genes – *BRCA1, BRCA2, PTEN, TP53, STK11, ATM, PALB2, CHEK2, RAD51C, RAD51D* and *BRIP1.* The two healthy individuals were VUS-carriers in *BRCA1* gene for the same variant. The VUS found in this population enrolled in the study is a missense, it changes an *A* to a *G* (forward – FW) and a *T* to a *C* (reverse – RV). Due to this modification, an arginine is produced instead of a glutamine. Although these patients do not have cancer, they do have family history with high occurrence of cancer. Furthermore, two different *in silico* prediction tools have distinct prognostics for the VUS, in PolyPhen2, it is probably damaging (0.998) (*PolyPhen 2*, 2020), whereas in Clin Var it is benign (*ClinVar - NCBI*, 2020) (Table 2.1).

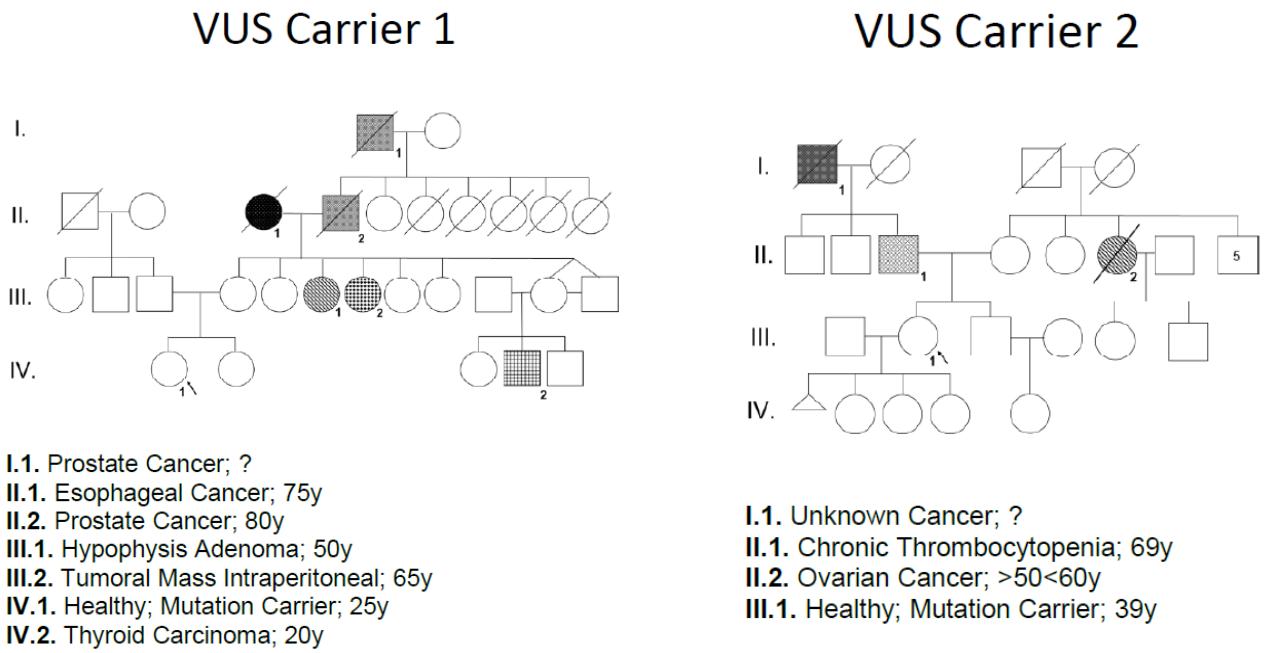

Figure 2.1 - Pedigree Diagrams and family history of samples VUS-carrier 1 and VUS-carrier 2.

Table 2.1 – Variants of unknown significance found in the population.

	Patients		
Age	25		39
Cancer	No		No
Gene	*BRCA1*		*BRCA1*
VUS	NM_007297.3:c.926A>G	NM_007294.3:c.1067A>G	NM_007294.3:c.1067A>G
EBI amino/genomic	ENSP00000350283.3:p.Gln356Arg 17:g.43094464T>C		ENSP00000418960.2:p.Gln356Arg 17:g.43094464T>C
rs	rs1799950		
Cons. Type	Missense		
PolyPhen	Probably damaging (0.969)		Possibly Damaging (0.795)
Clin Var	Benign		

2.2. Cell Culture

2.2.1. MCF10-A

MCF10-A cells were purchased from ATCC® (CRL-10317TM, Manassas USA). This is a human non-tumorigenic breast/mammary epithelial cell line. MCF10-A cells were cultured in Dulbecco's Modified Eagle Medium/F12 (DMEM-F12 - Sigma-Aldrich #D8437, Darmstadt Germany) supplemented with 5% horse serum (Sigma-Aldrich #H1270, Darmstadt Germany), 1% penicillin-streptomycin (with 10,000 units penicillin and 1 mg streptomycin per mL) (Sigma-Aldrich #P0781, Darmstadt Germany), 0.05% hydrocortisone (with a final concentration of 1 mg/mL) (Sigma-Aldrich #H0888, Darmstadt Germany) and 0.1% epidermal growth factor (EGF - Sigma-Aldrich #E9644, Darmstadt Germany). When treating the cells, choleric toxin pre-diluted 1:100 in double-distilled water - ddH2O (Sigma-Aldrich #C8052, Darmstadt Germany) with a final concentration of 100ng/mL and 10µg/mL of insulin (Sigma-Aldrich #I016, Darmstadt Germany) were added to the medium since neither of them can be frozen. The cell line was incubated at 37°C with 5% CO_2 in a humidified chamber.

2.2.2. MCF-7

MCF-7 are a human tumorigenic breast epithelial cell line. The cell line was purchased from DSMZ – German Collection of Microorganisms and Cell Culture GmbH (DSMZ no ACC 115, Germany). MCF-7 were cultured in Low Glucose DMEM (Sigma-Aldrich #D6046, Darmstadt Germany) containing with 10% of fetal bovine serum (FBS – Sigma-Aldrich #F7524), 2nM glutamine and 1% penicillin-streptomycin (with 10,000 units penicillin and 1 mg streptomycin per mL). When treating the cells, 10µg/mL of insulin was added to the medium. This cell-line is incubated at 37°C with 5% CO_2 in a humidified chamber.

2.3. Cell lines DNA extraction and sequencing

MCF10-A and MCF-7 cell lines were grown in culture flasks, until they reached the necessary confluence - 70-90% - for being trypsinised with 10% trypsin trypsin solution from porcine pancreas (Sigma-Aldrich #T4549, Darmstadt Germany) and versene plus sodium bicarbonate (sodium bicarbonate 8.4% BRAUN #304494, Kronberg, Germany). The cells were centrifuged at 800rpm for 5 min, then resuspended with the respective medium, obtaining a cell suspension of < $5x10^6$, which was used to extract the DNA of the cell lines using the AllPrep DNA/RNA mini kit (QIAGEN #80204, GmbH Germany), according to the manufacturer's instructions. Briefly, the samples were first disrupted and homogenised with the RLT buffer. Next, the lysate was transferred to a DNA column for purification with the addition of AW1, AW2 and EB buffers with multiple centrifugation steps amid. Finally, it was stored at 4°C until needed again. All samples were quantified using a NanoDrop™ spectrophotometer (Thermo Fisher, Darmstadt Germany).

PCR were performed with the DNA extracted, 5x MyTaq™ Reaction Buffer (Bioline #Bio-21106, GmbH Germany), MyTaq™ DNA polymerase 5U/µL (Bioline #Bio-21106, GmbH Germany), , forward primer (5' AGCCTGGCTTAGCAAGGAGC 3' – 60.1°C), reverse primer (5' TGGGGAGGCTTGCCTTCTTC 3' – 59.9°C) and ddH2O up to 50µL for 35 cycles using a thermocycler (AppliedBiosystem 9700, Foster City, California, United States) with five different cycling conditions: denaturation for 90 s at 94°C, annealing for 30 s at 60°C, extension for 30 s at 72°C and final extension for 10 min at 72°C.

PCR products were applied in a 1% agarose (Bioline #Bio-41025, GmbH Germany) gel, and the electrophoresis was performed at 70V for 1 hour, using the HyperLadder IV™ 100bp marker (Bioline, GmbH Germany). They were posteriorly stained with 3x GelRed (GelRed 10000x Biotium #41003, GmbH Germany) for 20 min and observed through ChemidocTM (Bio-Rad, GmbH, Germany). Each sample was performed in triplicate, and the results were confirmed twice in independent experiments.

The PCR samples were then purified using the GeneJET™ PCR Purification Kit (Thermo Fisher #K0701, #K0702, Darmstadt Germany) according to the manufacturer's instructions. Briefly, in between centrifugations, the binding, wash, and elution buffers were added to a DNA column in order to purify the PCR samples. The samples were then stored at -20°C. Beside the PCR, this cell line also had its *BRCA1* gene partially sequenced (~489bp) by STAB VIDA, in order to assure the MCF10-A and MCF-7 cell lines did not have the VUS.

2.4. CRISPR-Cas9

We used CRISPR-Cas9 as the genome-editing tool to introduce the VUS previously identified in the population into the MCF10-A and MCF-7 cell lines, making it either homozygous or heterozygous regarding the VUS. In previous studies by Pires, J.M., the protocol of plasmid transfection CRISPR-Cas 9 into the cell-lines was developed, based on Ran *et al, 2013*.

2.4.1. Design of single guide RNA and single-stranded DNA oligonucleotides:

Firstly, we designed the sgRNA and the ssODN using CRISPOR. This is an online CRISPR design tool that takes an input sequence and identifies and ranks the most fitting target sites, plus computationally forecasts off-target sites for each target. As such, it was possible to designe custom sgRNA (Table 2.2), as well as homology arms of 70 nucleotides on either side for optimal HR efficiency (Table 2.3). Afterwards, the ssODN was resuspended and diluted to a final concentration of 10µM and stored them at -20°C.

Table 2.2 - sgRNA designed for the VUS of interest using CRISPOR.

sgRNA	
Forward primer (FW) – 60.0°C	5' GAGATACTGAAGATGTTCCT*TGG* 3'
Reverse primer (RV) – 59.8°C	5' CTGCTATTTAGTGTTATCCA*AGG* 3'
GAGATACTGAAGATGTTCCTTGG 186 FW	
CTGCTATTTAGTGTTATCCAAGG 186 RV	

2.4.2. Transformation, delivery of sgRNA and repair template (ssODN);

The plasmid pSpCas9(BB)-2A-GFP (pX458) was transformed into a competent *E. coli* DH5α strain, according to the protocol supplied with the cells (NZYtech; MB12001) (Annex 1 – Figure 6.1). 5 to 10 µL of the DNA was added for the transformation. The mixture was then incubated on ice for 30 minutes, heat-shock at 42°C for 40 seconds and returned immediately to ice for 2 minutes. Next, we added 900µL of SOC medium and plated onto LB (BACTO AGAR BD #214030, Darmstadt Germany) plate containing 100µg/ml ampicillin and then incubated overnight at 37°C. By the next day, the inoculated cells were used to prepare the culture for the miniprep with LB medium and ampicillin 50mg/mL, which were incubated at 37°C 220rpm for 16 h. The plasmid culture were ready for the GeneJET™ Plasmid Miniprep Kit (Thermo Fisher #K0502 and #K0503, Darmstadt Germany). In short and according to the manufacturer's instructions, the ressuspension solution, lysis solution and neutralization solution

were added to the bacterial cell pellet in between mixing by inverting the tube. The lysate was then transferred to a GeneJET™ spin column where the Wash buffer was added two times between centrifugations. Ultimately, the Elution buffer, pre-warmed at 60°C, was added, and the eluted plasmid DNA was stored at -20°C.

For the top and bottom strands of sgRNA oligos were resuspended for each sgRNA design to a final concentration of 100 µM. Afterwards, was prepared a mixture for phosphorylating and annealing the sgRNA oligos (Table 2.4). Using a thermocycler (AppliedBiosystem 9700, Foster City, California, United States), the oligos were phosphorylated and annealed with the following parameters: 37°C for 30 min; 95°C for 5 min; and finally ramp down to 25°C at 5°C.min-1. The phosphorylated and annealed oligos were diluted in a ratio 1:200 in ddH_2O.

Table 2.3 - Oligos and ssODN 140 nucleotides homology arms designed for the VUS of interest using CRISPOR.

Oligos and ssODN homology arms
FW Oligo 1→5' – CACC**GAGATACTGAAGATGTTCCT** - 3' 3' - **CTCTATGACTTCTACAAGGA**CAAA – 5' ← Oligo 2 **RV** Oligo 1→5' –CACCG**CTGCTATTTAGTGTTATCCA** - 3' 3' - C**GACGATAAATCACAATAGGT**CAAA - 5' ← Oligo 2
ssODN homology arms (140nt) ACTCCCAGCACAGAAAAAAAGGTAGATCTGAATGCTGATCCCCTGTGTGAGAGAA AAGAATGGAATAAGC**G**GAAACTGCCATGCTCAGAGAATCCTAGAGATACTGAAGA TGTTCCGTGGATAACACTAAATAGCAGCAT

Table 2.4 - Phosphorylation and annealing of sgRNA oligos.

Components
sgRNA top (100 µM) (STAB VIDA)
sgRNA bottom (100 µM) (STAB VIDA)
T4 reaction buffer, 10x (Thermo Scientific EK0031, Darmstadt Germany)
T4 polynucleotide kinase – PNK, 10 U/µL (Thermo Scientific EK0031, Darmstadt Germany)
ddH2O (up tp 10µL)

Then, the sgRNA oligos were cloned into the pX458 plasmid and set up a ligation for each sgRNA, as described below. A no-insert pX458-only was used as a negative control for the ligation (Table 2.5). The ligation reaction was incubated for a total of 1h.

The plasmid with the insertion of sgRNA was transformed into a competent *E. coli* DH5α strain, as previously described. From each transformed plate, 2 to 3 colonies were chosen to verify if the sgRNA was inserted correctly. The cultures were incubated with LB medium at 37°C 220rpm for 16 h. Next, the plasmid culture were ready for the GeneJET™ Plasmid Miniprep Kit according to the manufacturer´s instructions.

In order to verify the correct insertion of the sgRNa in the plasmid, we performed a double digestion with two restriction enzymes, BpiI and BshTI (Thermo Scientific #FD1014 and #FD1464, Darmstadt Germany, respectively), following the conditions below (Table 2.6). The double digestion was then run in a 1% agarose gel with the HyperLadder™ 1kb marker (Bioline, GmbH Germany). pX458 sgRNA was used as the positive control for the correct insertion of the sgRNA, whereas the no-insert pX458 was used as the negative control.

Table 2.5 - Cloning of sgRNA into pX458 plasmid and no-insert sgRNA pX458.

Components	
pX458 (100 ng)	
Diluted oligo duplex, 1:200	
Tango buffer, 10x	
Dithiothreitol - DTT, 10 mM (Thermo Scientific R0861, Darmstadt Germany)	
ATP, 10 mM (Thermo Scientific R0441, Darmstadt Germany)	
FASTDigest BpiI (Thermo Scientific FD1014, Darmstadt Germany)	
T4 ligase (Thermo Fisher K1422, Darmstadt Germany)	
ddH2O (up to 20µL)	
Cycle number	**Condition**
1-6	37°C for 5 min, 21°C for 5 min

The ssODN were inserted into the pX458 sgRNA and pX458 without sgRNA in a ratio of 4:2 (4µL of ssODN template – 10 µM – to 2µg of pX458 with sgRNA and pX458 without sgRNA).

The stocks of each plasmid, no-insert pX458-only and pX458 with the insertion of sgRNA, were prepared with 10% glycerol (Glycerol 85% MERK #Z0404394640, Darmstadt Germany), LB medium and ampicillin 50mg/mL. Before they were stored at -80°C, all samples were quantified using a NanoDrop™ spectrophotometer.

Table 2.6 - Double digestion with BpiI and BshTI fast digestion enzymes.

Components	
pX458 with and without sgRNA (200ng)	
FASTDigest BpiI (1µL)	
FASTDigest BshTI (1µL)	
FASTDigest buffer, 10x (2µL)	
ddH2O (up to 20µL)	
Conditions	
Reaction	Inactivation
37° C for 30 min	80°C for 10 min

2.4.3. Transfection, isolation and single-cell cloning after selection;

MCF10-A and MCF-7 cell lines were co-transfected with the transformed plamid pX458 with sgRNA and ssODN and no insert pX548 ssODN in a ratio of 1:2 and 1:3 with cationic polymer polyethylenimine (PEI; for example, 9µL of PEI to 3µg of plasmid DNA). As for the positive control for the transfection, we use pmaxGFP in the same ratio as the plasmid, whereas non-treated cells were used as the negative control.

After 48 to 72h, the GFP positive clones were sorted one by one through flow cytometry using FACS Aria III™ (BD Biosystem, Franklin Lakes, New Jersey) into a 96-well plate with respective supplemented medium for each cell line. The cells were then incubated at 37°C with 5% CO_2. As far as the cells had reached a confluent level, they were passed into a new 24-well plate with appropriate medium and incubated typically until confluence. The cell growth and maintenance procedure were performed and guaranteed through several new passages respecting an increasing area of plates and flasks size (e.g. 12-well plate; 6-well plate; T25; T75 flasks and T175 flasks).

2.4.4. Confirm point mutation through PCR and sequencing.

The cells were grown in culture flasks until reaching the necessary confluence, after trypsinisation a cell suspension of < $5x10^6$ was obtained, which was used to extract the DNA of the cell line using the AllPrep DNA/RNA mini kit, as previously described. All samples were quantified using a NanoDrop™ spectrophotometer.

PCR were performed with the same mixture and cycling conditions as the ones presented in section 2.2. Then, the PCR products were applied in a 1% agarose gel, and the electrophoresis was performed at 70V for 1 hour, using the HyperLadderIV™ 100bp marker. They were posteriorly stained with 3x GelRed for 20 min and observed

through Chemidoc™. Each sample was performed in triplicate, and the results were confirmed twice in independent experiments. The PCR samples were then purified using the GeneJET™ PCR Purification Kit, also previously described.

Finally, the *BRCA1* gene was partially sequenced in the cell lines by STAB VIDA through Sanger sequencing, in order to confirm if the MCF10-A transfected and MCF-7 transfected cell lines have indeed the VUS of our interest.

2.5. Single-cell gel electrophoresis – Comet assay

Single cell gel electrophoresis (SCGE) or comet assay is a simple, rapid and sensitive method for detecting DNA damage in individuals' cells (Collins, 2004; Kumaravel *et al.*, 2009; Nandhakumar *et al.*, 2011; Singh *et al.*, 1988). It allows to detect low levels of DNA damage, such as DNA SSB/DSB and alkali-labile sites (apurinic/apyrimidinic sites), as well as alkylation damage and oxidised bases. SCGE has become one of the standard methods in genotoxicity testing, human biomonitoring, ecogenotoxicology, as well as fundamental research in DNA damage and repair (Collins, 2004; Nandhakumar *et al.*, 2011; Olive e Banáth, 2006). In short, cells are immersed in agarose on a microscope slide and then lysed with a detergent. They are submitted to high pH electrophoresis, and the result is a shape that resembles comets, observed through fluorescence microscopy, which means there is a need for DNA staining, like a DNA intercalating agent, such as GelRed. The intensity of the comet's tail and head are measured and compared, giving the number of DNA breaks with the percentage of DNA in the tail. This technique is based upon that DNA fragments of single-cell nuclei, which are negatively charged, move towards the anode, during electrophoresis by losing their supercoiling (Collins, 2004; Olive e Banáth, 2006) The comet assay was performed under alkaline conditions as reported by Singh *et al.* (1988). This version, using a lysis solution and a non-ionic detergent, allows the cell membrane, cytoplasm and nucleoplasm to be removed, leaving just the nucleoid, which is treated with a high alkaline solution (pH > 13). This allows the DNA supercoils to unwind, thus revealing the alkali-labile sites, or breaks. These breaks migrate towards the anode when submitted to an electric current, hence producing a "comet-like" structure.

Both cell lines were grown in flasks until confluence was reached; they were trypsinised with 10% trypsin, versene plus sodium bicarbonate. Cells were centrifuged at 800rpm for 5 min, then resuspended obtaining a cell suspension of $1x10^5$ cells per well. The cells were incubated into a 6-well plate at 37°C with 5% CO_2 with supplemented respective medium where they were exposed to a variety of genotoxic agents with different concentrations (Doxorubicin (Fisher Bioreagents, Darmstadt

Germany) - DOX 0.1μM, 1μM, 2.5 μM and 5μM; Hydrogen peroxide (MERK #K44653709335, Darmstadt Germany) - H_2O_2 50μM) for one hour and a half. Non-treated cells were used as a negative control (NC), while cells treated with H_2O_2 were used as a positive control. Afterwards, the medium was removed, and the cells were washed with versene plus sodium bicarbonate.

The cells were then trypsinised. DPBS (Gibco #14190-094, Darmstadt Germany) was added, and the cells were then centrifuged at 1100 rpm for 5 min at 4°C. They were then rinsed with PBS (Sigma-Aldrich #P-3813, Darmstadt Germany) and centrifuged once more under the same conditions. Subsequently, the cells were dissolved in 0.5% low melting point (LMP) agarose (Sigma-Aldrich #A9414-5G, Darmstadt Germany) and spread onto a microscope slide pre-coated with 1% normal melting point (NMP) agarose (Bioline #Bio-41025, GmbH Germany) where they were incubated with coverslips for 20 min at 4°C. The coverslips were removed, and the slides were left in a coplin jar covered with aluminium overnight on a cold lysis solution (2.5M sodium chloride – NaCl Fisher Bioreagents #S/3120/60, Darmstadt Germany) -, 10mM trisaminomethane - Tris base (Fisher Bioreagents #BP152-500, Darmstadt Germany), 100mM Ethylenediaminetetraacetic acid - EDTA 99% (Sigma Aldrich #EC205-358-3, Darmstadt Germany), 1% Triton X-100 (Sigma-Aldrich #9002-93-1, Darmstadt Germany), pH 10).

By the next day, the slides were washed with cold water and remained soaked in it for 10 min at 4°C. They were then dipped in fresh electrophoresis buffer (10M sodium hydroxide - NaOH (Acros Organics #447280050, Darmstadt Germany), 200mM EDTA, pH > 13) for 20 min at 4°C, enabling the unwinding of the DNA. Electrophoresis ran for 20 min at 25V (400mA). Subsequently, the slides were neutralised (0.4M Tris, pH 7.0) three times for 5 min, dried with ethanol (ethanol absolute MERK #K45611583424, Darmstadt Germany) (50%, 75% and 90%, one time, 5 min each) and on a hot plate for about 20 to 30 min. Before heading to the microscope, the slides were stained with 3x GelRed and covered with coverslips. The cells were acquired with a 200x amplification from a fluorescent microscope (Zeiss Z2).

To randomly assure the selection of approximately 225 cells of each treatment, 35 fields were chosen and captured. The cells were then analysed by the CometScore™ v1.5 software. The percentage of DNA in the tail (% DNA in tail) of the comets was measured in order to assess the extent of DNA damage.

2.6. ɣ-H2AX flow cytometry

DNA is enfolded around a core histone molecule forming the nucleosome complex. Histone H2AX belongs to H2A family, responsible for packaging and organizing eukaryotic DNA into chromatin. As soon as a DSB occurs into the DNA, H2AX it is almost immediately phosphorylated at serine 139 at the C-terminus, delineating the DSB in the chromatin; the phosphorylation of H2AX is named γ-H2AX (Georgoulis *et al.*, 2017; Kopp, Khoury e Audebert, 2019). γ-H2AX is considered critical in DDR, not only it is mediated by main player from the DNA DSB repair pathways, like ATM, ATR or DNA-dependent protein kinase (DNA-PK) (Georgoulis *et al.*, 2017). But also, it promotes stable accumulation of many other signalling and repair proteins, including BRCA1 at DSB sites. Additionally, it has been shown that the number of γ-H2AX focal sites in cell nuclei corresponds to the number of DSB (Firsanov *et al.*, 2017) Hence, this protein can be considered a sensor, present in the initial recognition checkpoints of DNA damage (Kopp, Khoury e Audebert, 2019).

ɣ-H2AX can be measured either through immunofluorescence since it forms green nuclear foci on the chromatin, which represents a DSB; thus, providing the extent of the damaged DNA in the nucleus (Huang e Darzynkiewicz, 2006). Instead, by flow cytometry, it allows a quick and more sensitive quantification of DNA damage on a large cell population. (Huang e Darzynkiewicz, 2006; Kopp, Khoury e Audebert, 2019). This method provides a reliable estimate of DNA damage in a vast number of cells (Firsanov *et al.*, 2017). The detection of ɣ-H2AX is founded upon indirect immunofluorescence using a secondary antibody tagged with fluorescein isothiocyanate (FITC), whereas DNA is counterstained with propidium iodide (PI). The cytometer will measure the intensity of green (FITC) and red (PI), thus reporting the extent of the damaged DNA, regarding the frequency of DSBs (Huang e Darzynkiewicz, 2006).

MCF10-A and MCF-7 cell lines were grown in flasks, a cell suspension of $1x10^6$ cells per well was obtained. The cells were incubated in a 12-well plate at 37°C with 5% CO_2 with supplemented respective medium where they were exposed to diverse drugs with different concentrations (DOX 0.1μM, 1μM and 5μM; Hydrogen peroxide - H_2O_2 25μM, 50μM and 100μM) for two hours. Non-treated cells were used as a NC, whereas cells treated with DOX 5μM were used as a positive control.

Afterwards, the medium was removed, and a new medium was added for cells to recover from the genotoxic challenge for 40 min. Next, the medium was removed once more, and the cells were rinsed with PBS and trypsinised (Gibco #A1110501, Darmstadt Germany). PBS was added, and the cells were centrifuged at 1100rpm for

5 min at 4°C. Afterwards, they were incubated with PBS and stained with LIVE/DEAD fixable violet dead cell stain kit (Invitrogen L34955, Darmstadt Germany) for 30 min at room temperature, protected from light. Later, cells were rinsed with PBS, centrifuged again and incubated for 15 min on ice with formaldehyde 2% (formaldehyde 16% - Thermo Fisher #28906, Darmstadt Germany - PBS). They were once again centrifuged and fixed overnight with cold ethanol 70% (PBS and Ethanol 100%).

By the next day, cells were centrifuged anew and washed with blocking solution (BSA – Sigma Aldrich #A4503-50G, Darmstadt Germany -, PBS, goat serum – Sigma-Aldrich #G9023, Darmstadt Germany - Triton X-100), then centrifuged again and incubated two hours with conjugated antibody Anti-Hu/Mo Phospho-histone H2AX (Ser139) with PI (Invitrogen #12-9865-42, Darmstadt Germany) at room temperature, protected from light. Next, cells were rinsed with BSA 1% (BSA 4% and PBS). Another centrifugation and cells were finally resuspended with BSA 0.1% (BSA 1%, PBS). The results were acquired with FACS CANTO II™ and processed with the FlowJo™10 software.

2.7. Annexin V

Apoptosis is a programmed cell death; this is considered vital in multiple cells processes. One in particular, is on damaged cells resulted from external or internal factors, or even diseases like cancer. Annexin V is a recombinant phosphatidylserine-binding protein that has a strong Ca^{2+} dependent affinity and specifically with anionic phosphatidylserine residues (PS). Normally, PS is located on the cytoplasmic surface of the plasma membrane, but during apoptosis a translocation of the PS occurs to the outer leaflet or extracellular side of the plasma membrane. Since Annexin V interacts with PS it can be used as a probe for apoptosis (Elmore, 2007). PI is commonly used to indicate cell viability; thus when used in conjunction with Annexin V is possible to distinguish viable, apoptotic or necrotic cells through differences in plasma membrane integrity and permeability (Elmore, 2007; Rieger *et al.*, 2011). Once the apoptotic cells are bound with FITC-labeled Annexin V, they can be visualized with flow cytometry.

All cell lines were grown in flasks, a cell suspension of $1x10^6$ cells per well was obtained. The cells were incubated in a 12-well plate at 37°C with 5% CO_2 with supplemented respective medium where they were exposed to DOX 0.1µM, 1µM and 5µM, H_2O_2 25µM, 50µM and 100µM, and camptotecin (CPT) 5 µM as a positive control for apoptosis, for four hours. Next, the cells were trypsinised. PBS was added, and the cells were then centrifuged at 1100 rpm for 5 min. They were then rinsed with PBS and

centrifuged once more under the same conditions. Thereafter, it was incubated with conjugated FITC-Annexin V (Thermofisher Scientific #A13199 – Eugene, Oregon USA), with PI (Thermofisher Scientific #P3566, Eugene, Oregon USA) for 15min, protected from the light and at room temperature. Finally, the results must be acquired in the next hour. These were obtained with FACS CANTO II™ and processed with the FlowJo™10 software.

2.8. Western Blot

Western blotting is a common technique used to detect proteins. This rapid and sensitive assay separates and identifies proteins based on their molecular weight through gel electrophoresis. Briefly, the results obtain in the electrophoresis are then transferred to a membrane producing a band for each protein, being then incubated with specific antibodies for the protein of interest. The unbound antibody is washed off leaving only the bound antibody to the protein, these are then detected by developing the film. Due to its specificity, only one band is expected. Furthermore, the thickness of the band corresponds to the amount of protein present; hence, using a standard can indicate the amount of protein present (Mahmood e Yang, 2012; Mishra, Tiwari e Gomes, 2017).

All cell lines were grown in culture flasks, until reached the optimal confluence for being being trypsinised. The cells were centrifuged at 800rpm for 5 min, then resuspended with the PBS (Sigma-Aldrich #P-3813, Darmstadt Germany), obtaining a cell suspension of < $5x10^6$. Next, the cell suspension was centrifuged at 500rpm for 10min ate 4°C and rinsed again with PBS and centrifuged once more under the same conditions. Afterwards, a lysis tampon containing Buffer C 10X (Tris-base 50nM ph=8, 150mM NaCl and 5mM EDTA), Nonidet P-40, PMSF 0,1M and Protease Cocktail 7x was added in a proportion of 25µL to $1x10^6$ cells and then let incubate for 30 min on ice. Lastly, centrifuge the sample at 14000g for 10min ate 4°C, remove and store the supernatant at -80°C. For protein quantification we used the Bradford method. This is an easy and quick procedure that enables processing a large number of samples; the protein-dye complex has a high extinction factor leading to a considerable sensitivity in measurement of the protein. It is based on the fact that Coomassie Brilliant Blue upon binding of the dye to the protein, occurs it the convert red into blue (Bradford, 1976). A Bovine Serum Albumin (BSA) solution of 2 mg/ml (Bio-Rad, USA #500-0206) was used to prepare a calibration curve, with different dilutions (0 µg, 1 µg, 2 µg, 4 µg, 8 µg, 16 µg and 32 µg). The samples were diluted in 1:400 ratio in ddH_2O. Then, the Bradford reagent (Bio-Rad, #500-0006 USA) was added in 1:5 ratio. All the

prepared dilutions and samples were transferred to a 96-well plate and their absorbance was read at 595 nm (SpectraMax i3x plate reader, Molecular Devices, USA).

For the Western Blot, an equal amount of protein from each sample (10µg) was dilute 1:1 with Loading buffer 2X (Loading buffer 5X – SDS 10%, Glycerol 50%, Bromophenol blue 1%, Tris-HCl 1M and ddH_2O; with final pH 6.8 – at the moment of use we add β – mercaptoethanol 1:10) to a final volume of 10µL and then heated in a dry plate for 5 min at 95°C. The proteins were concentrated on 5% sodium dodecyl sulfate polyacrylamide gel electrophoresis (SDS-PAGE) and resolved on 10% SDS-PAGE gel. The electrophoresis was performed at 60V for 15min or until all samples enter the resolution gel, then we changed to 100V for 1 hour and a half. The PVDF membrane was activated for 5-10s in methanol. The blotting was performed for 1h at 100V. The blotted proteins were then incubated using primary antibody BRCA1 (GeneTex GTX70113 USA) and β-actin (GeneTex GTX629630 USA) was also used as control, both in a proportion of 1:1000 over-night. In the next day, the proteins were revealed with goat anti-mousse secondary antibody conjugated to streptavidin. Visualization of protein bands was observed through Chemidoc™.

2.9. Statistical analysis

Data were analysed with GraphPad Prim® 9.0.0 (GraphPad Software Inc., San Diego, CA, USA). Values are presented with an approximate mean ± standard error of the mean (SEM). In the comet assay, the statistical analysis of the assessed parameters was performed based on One-way ANOVA (parametric test) variance analysis with Dunn's multiple comparison test; where, when needed, comparison tests were applied; namely, the Wilcoxon Matched Pairs test (non-parametric test). In all assays, there was a level of statistical significance of 95% ($p<0.05$). In γ - H2AX flow cytometry, the statistical analysis was performed based on One-way ANOVA (parametric test) variance analysis with Dunnett's Multiple Comparison Test, with a level of statistical significance of 95% ($p<0.05$).

3. Results

Results

3.1. CRISPR-Cas 9

As stated before, we choose CRISPR-Cas9 methodology to introduce our VUS of interest into a human non-tumorigenic breast cell line – MCF10-A – and into a human tumorigenic breast cell line as a positive control – MCF-7.

Firstly, we had to ensure the delivery of sgRNA into pX458, so we did a double digestion with BpiI and BshTI, confirming if the clones chosen did indeed introduce the sgRNA, or not (Figure 3.1). Next, to introduce the VUS in the most precise way possible, which means through HR, a repair template (ssODN) was delivered into the pX458 sgRNA and the no-insert pX458. The cells were isolated, and clones were selected one by one through flow cytometry, due to their GFP expression, but only the ones comprising pX458 sgRNA ssODN (Figure 3.2).

Lastly, as soon as the clones reached enough confluence to extract the DNA, PCR (Figure 3.3) and sequencing (Figures 3.4 and 3.5) took place in order to confirm whether the VUS was indeed introduced into the MCF10-A and MCF-7 cell lines. Only MCF10-A had the VUS introduced with success.

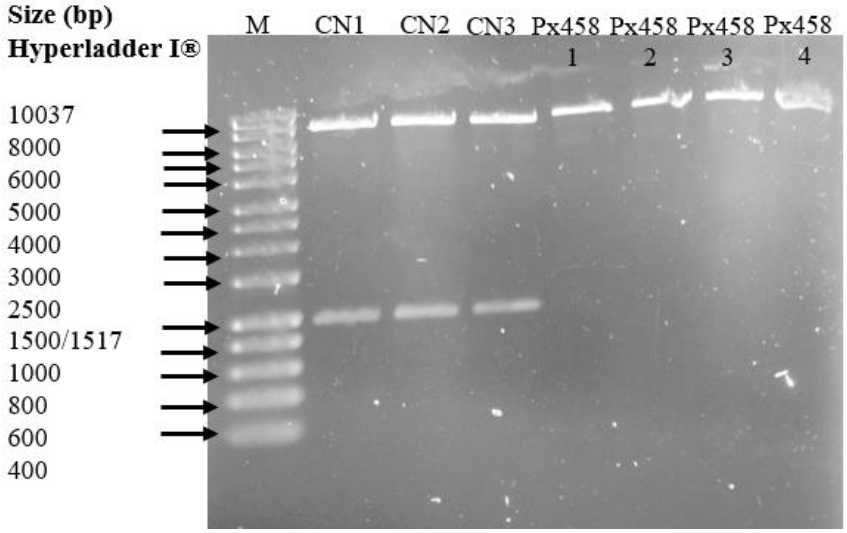

Figure 3.1 - Delivery of sgRNA. Double digestion with BpiI and BshTI, Clones with insertion will show only linearized plasmid of ~8.5 kb (only BshTI will be able to cut), whereas clones without insertion will show a ~1kb and ~7.5kb fragment (both BpiI and BshTI will be able to cut). The marker used was HyperladderTM 1kb (Bioline H1-211K). **Legend: CN** - negative control, no-insert into pX458**; M** – Marker; **Px458** – positive control, pX458 with sgRNA insert.

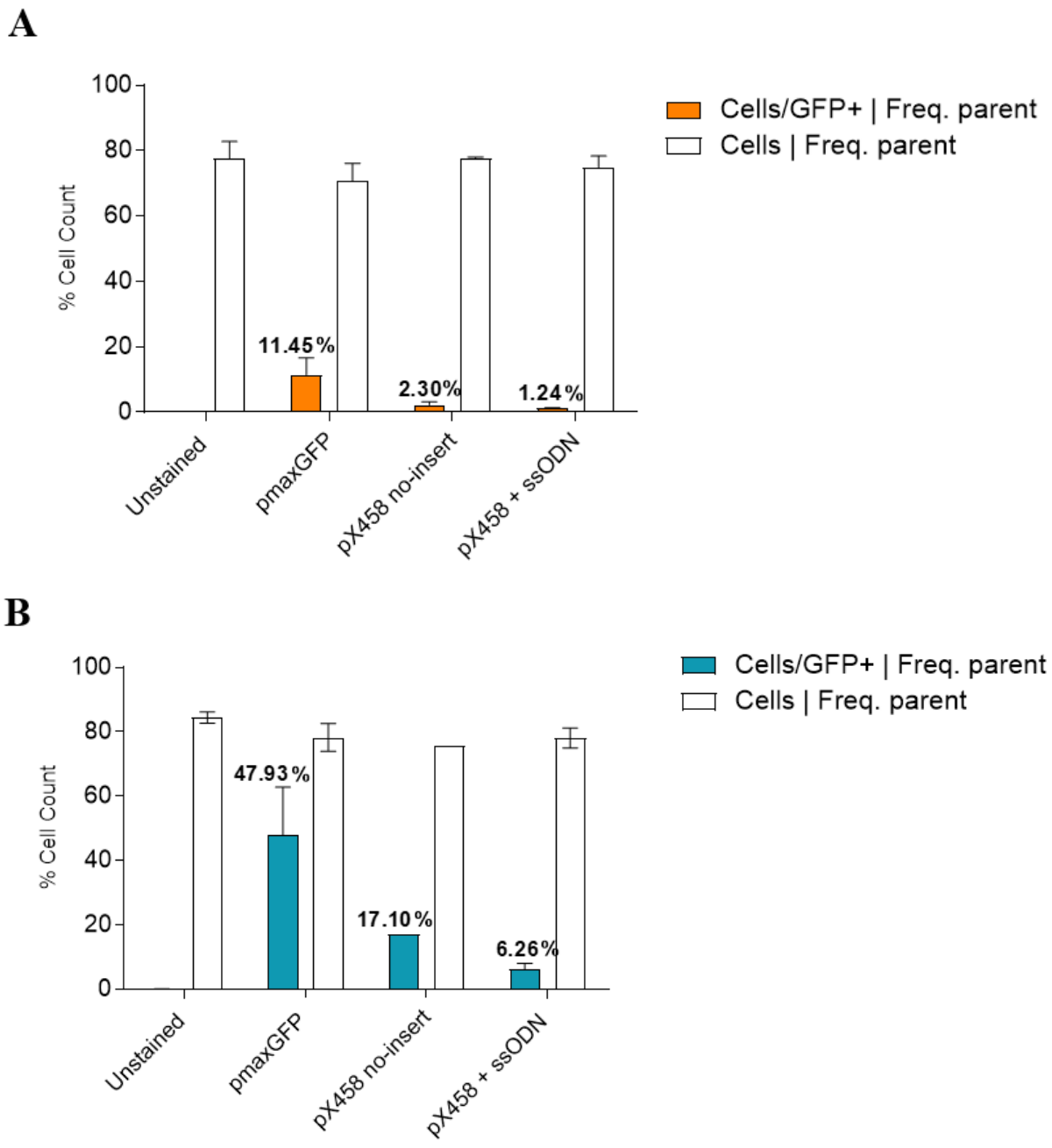

Figure 3.2 – Single-cell selection and isolation of clones from MCF10-A (A) and MCF-7 (B) cell lines. Percentage of GFP positive cells and frequency of the unstained, pmaxGFP and pX458.

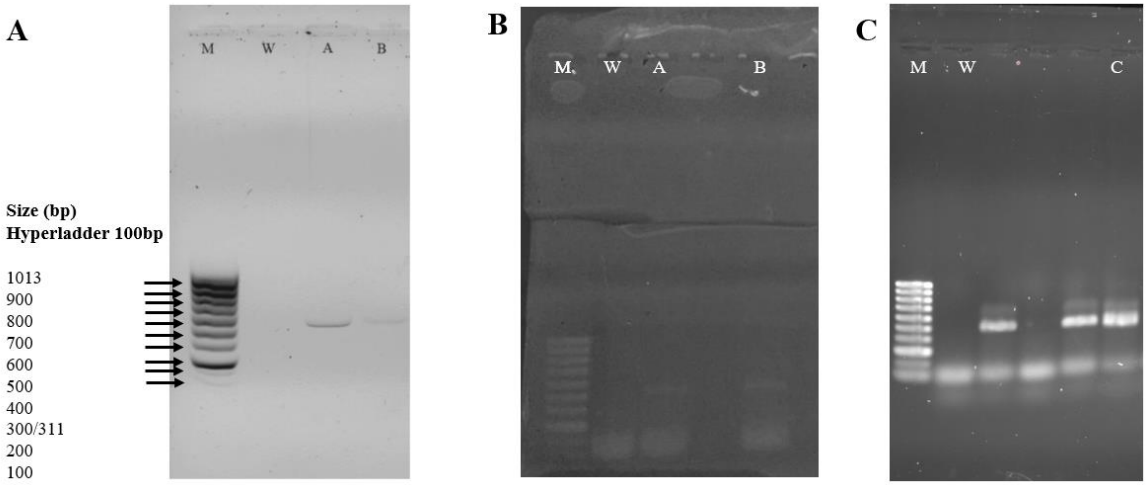

Figure 3.3 - Confirmed point mutation through PCR. A- PCR of non-tumorigenic MCF10-A cell. **B-** PCR of MCF-7 cell line. **C** – PCR of MCF10-A cell line with pX458 sgRNA ssODN, with our VUS of interest. All samples where posteriorly sent for sequencing. **Legend: W**- negative control; **M** - marker Hyperladder™ 100bp.**A, B and C**- both stand for the DNA samples extracted for the PCR of the respective cell lines.

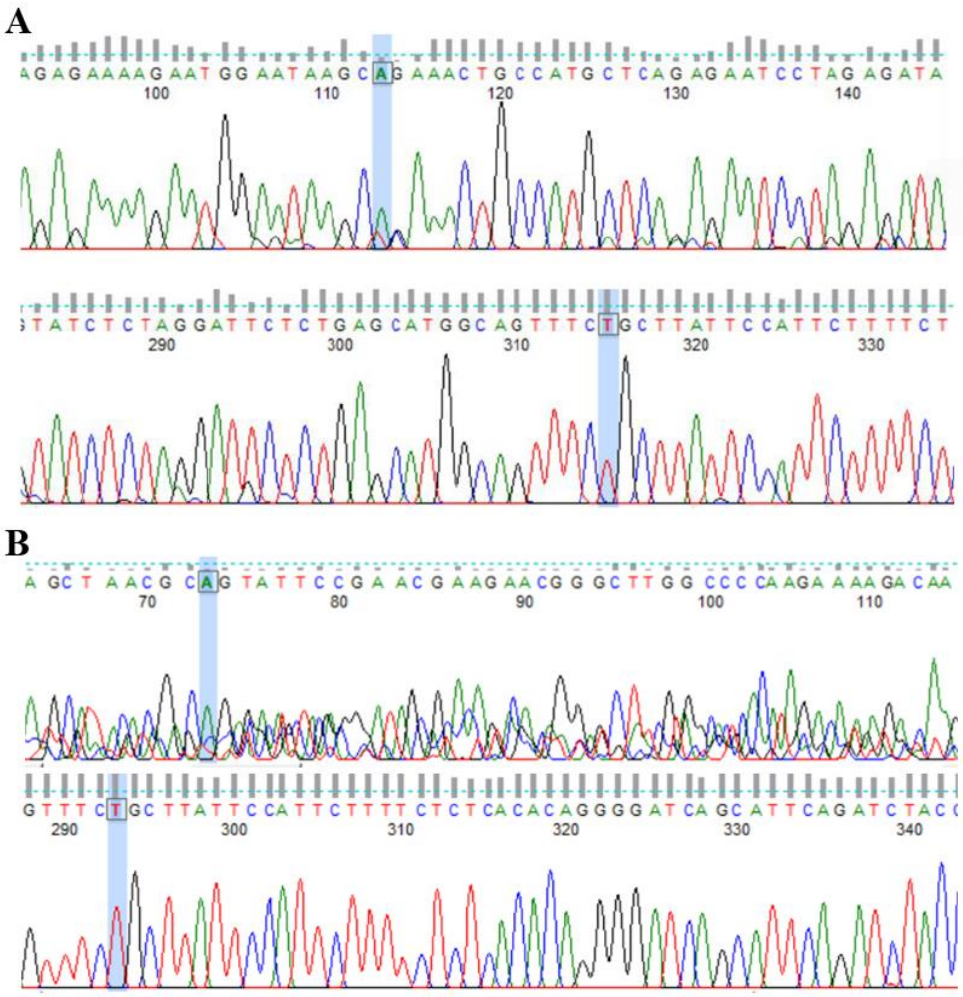

Figure 3.4 – Confirming point mutation through sequencing. A – Results from MCF10-A cell line. **B** – Results from MCF-7 cell line. The top image represents the forward sequence, while the bottom image represents the reverse sequence. Both cell lines have normal sequences: top – C**A**G; bottom – C**T**G

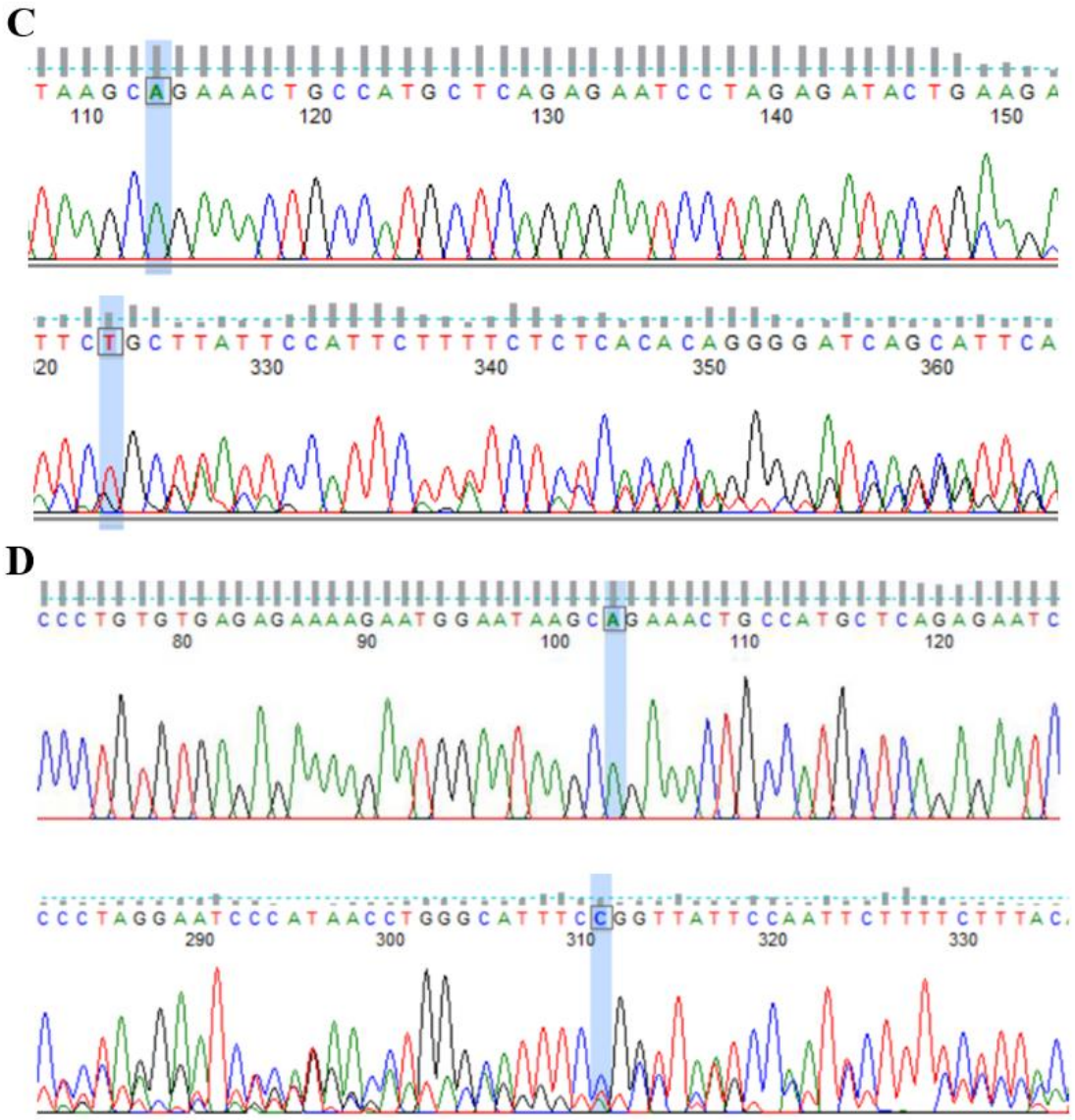

Figure 3.5 – Confirming insert of point mutation through sequencing. C and D results from MCF10-A with VUS cell line. The top image represents the forward sequence, whereas the bottom image represents the reverse sequence. The forward strand has the normal sequence, C**A**G; whereas the reverse strand have the point mutation wanted, C**C**G.

3.2. Single-cell gel electrophoresis – Comet assay

With this technique, it was possible to assess the DNA damage induced by DOX to MCF10-A, using this as a baseline for comparison to the DNA damage induced to the MCF-7 and MCF10-A cell line with the inserted VUS. The cell lines were exposed to a genotoxic challenge for 1h and a half, like this DNA repair mechanisms would not have enough time to initiate the reparation of the damage induced. For this assay, well established in our group, H_2O_2 50µM was used as our positive control, since it induces a high amount of DNA damage.

The results were obtained with Zeiss Z2 fluorescence microscope with 200x amplification. For each sample, 30 fields were captured, including duplicates, and 225 cells for each dose were randomly chosen. To measure the percentage of DNA in the "comets" obtained we use CometScore™ software (Figure 3.6). All statistical data regarding the overall response for MCF10-A, MCF-7 and MCF10-A with inserted VUS are represented in Figure 3.7. The analysis was made through GraphPad Prism 9 software using One-way ANOVA Dunn's Multiple Comparison Test (p-value < 0.05), where each treated sample was only compared to the NC. The distribution of %DNA in tail was plotted with a mean percentage ± SEM. Overall, statistical differences is showed merely between the NC and H_2O_2 50µM. MCF10-A, is the only cell line which all treatments have statistical significance. Whereas MCF10-A VUS besides our positive control, only presents one more treatment with statistical difference, DOX 5µM.

When comparing MCF10-A and MCF-7 treatments between each other (Annex 3 - Figure 6.3) and MCF10-A with MCF10-A VUS (Figure 3.8) the situation changes: all groups were statistically significant. It was used Wilcoxon Matched Pairs test (p-value < 0.05), where each sample distribution of % DNA in the tail was plotted with mean percentage ± SEM.

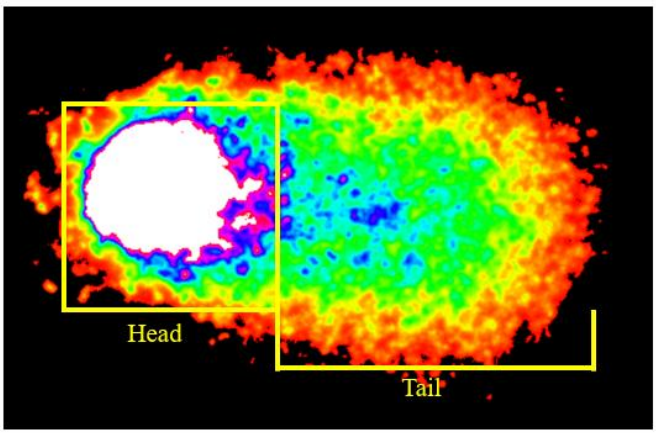

Figure 3.6- Representative image of fields captured for the comet assay. Obtained from MCF10-A cell line with inserted VUS when treated with H_2O_2 50µM using CometScore ™ software.

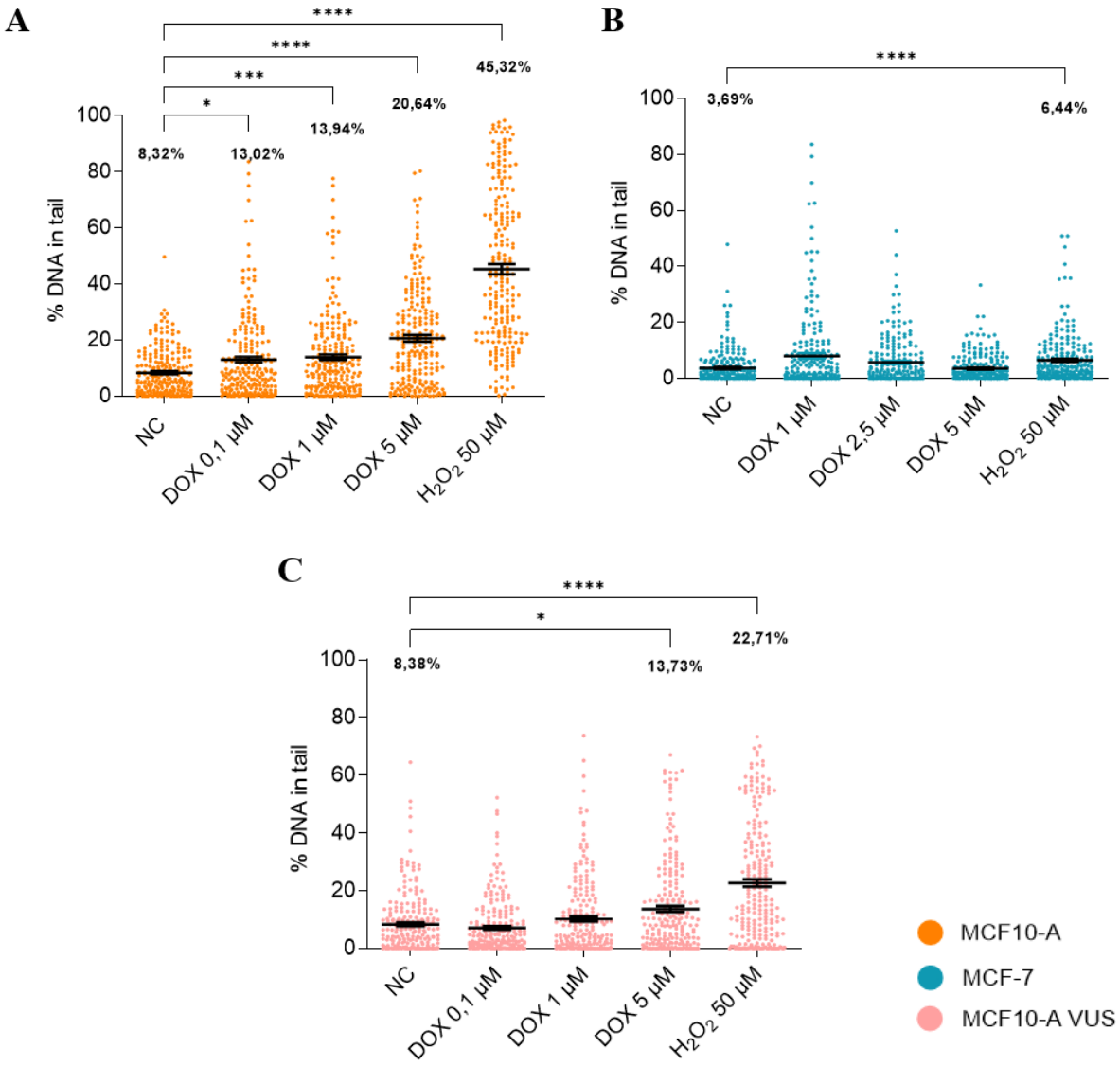

Figure 3.7 - % of DNA in tail in each treatment in all cell lines. Distribution % of DNA in tail was plotted for each sample and dose using GraphPad Prism 9 software with mean values ± SEM are represented by black lines. Statistical analysis with One-way ANOVA Dunn's Multiple Comparison Test and a p-value < 0.05 was considered statistically significant being represented with * - the number of * represents how relevant the statistical difference is. **A-** MCF10-A: all doses and samples showed statistically significant differences when compared with the **NC** (negative control). **B-** MCF-7: only presents statistically significant differences with our positive control H_2O_2 50µM. **C-** MCF10-A with inserted VUS: it shows statistically significant differences with DOX 5µM and as expected, with H_2O_2 50µM.

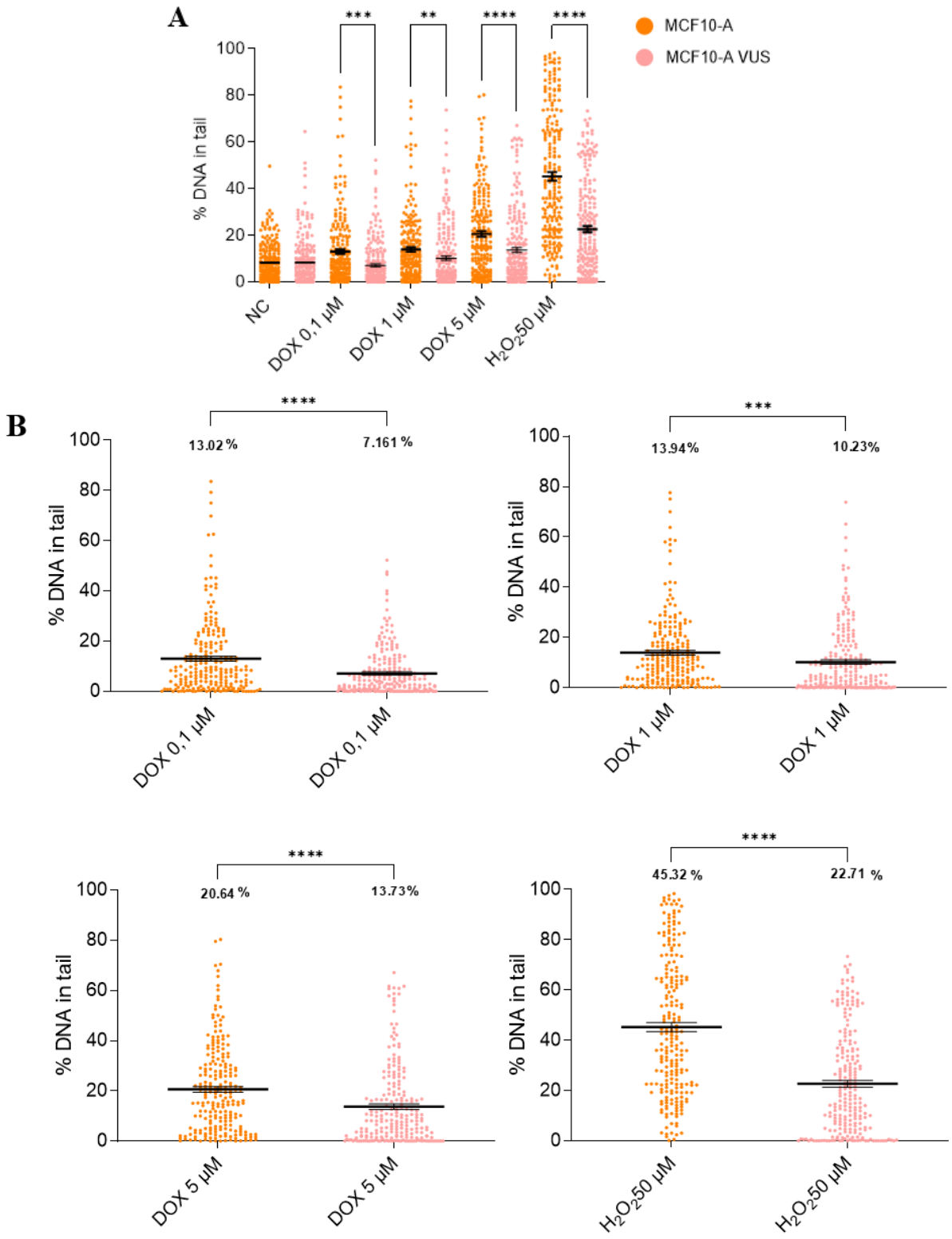

Figure 3.8 - % of DNA in tail in each treatment in MCF10-A versus MCF10-A VUS. A- Overall view of different treatments on MCF10-A against MCF10-A VUS. **B-** % of DNA in tail distribution was plotted for each sample and dose using GraphPad Prism 9 software. Mean values ± SEM are represented by the black lines. Statistical analysis with Wilcoxon Matched Pairs test and a p-value < 0.05 was considered statistically significant. Statistical significance is represented with * (the number of * represents how relevant is the statistical difference). All doses presented statistical significance differences, where MCF10-A has a higher % of DNA in tail when compared with the VUS cell line.

3.3. ɣ-H2AX flow cytometry

To have a more insightful and specific evaluation of the DNA damage which was induced, and to better corroborate the data from the comet assay, we performed ɣ-H2AX flow cytometry. With this assay, we measure DNA DSBs, whereas in the previous assay we measure all type of damage. More importantly, in this assay our positive control is DOX 5µM since it is known to create DSBs. H_2O_2 would not be the most appropriate candidate for positive control, since it creates DNA damage through the formation of ROS, resulting in lesions that may not be DSBs.

The results were obtained from FACS Canto II cytometer where approximately 20000 cells were collected for each treatment (Annex 2 - Figure 6.2). After which, they were analysed by FlowJo™ 10 software, to obtain the percentage of ɣ-H2AX in each treatment (Figure 3.9). As expected, all cell lines had statistically significance DNA damage with DOX 5µM against our NC. Also, MCF10-A and MCF-7 displayed significant differences with DOX 1µM. As we compare the different doses and drugs between cell lines: MC10-A versus MCF-7, DOX 1µM, DOX 5 µM and H_2O_2 50µM presented statistical significance differences (Annex 4 Figure 6.4). When comparing MCF10-A and MCF10-A VUS, only DOX doses presented statistically significant differences (Figure 3.10).

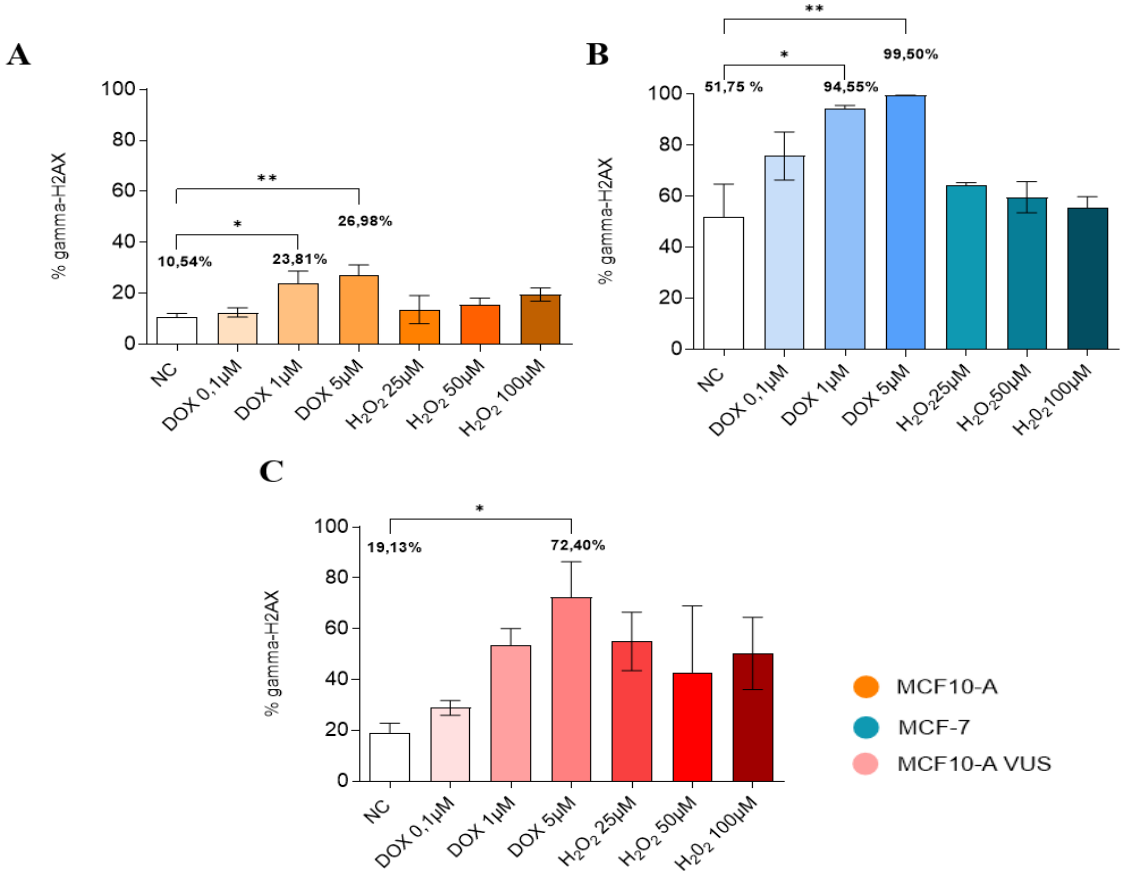

Figure 3.9 - Overall % of ɣ-H2AX in each drug exposure of all cell lines. A- % of ɣ-H2AX in each drug exposure in MCF10-A cell line; **B -** % of ɣ-H2AX in each drug exposure in MCF-7; **C** - % of ɣ-H2AX in each drug exposure in MCF10-A VUS. The graphs were plotted using GraphPad Prism 5 software. Mean values ± SEM are represented by error bars. Statistical analysis with Dunnett's Multiple Comparison Test and a p-value<0.05 was considered statistically significant. DOX 1µM and DOX 5µM statistically significant to their negative control (NC) in all cell lines, except for MCF10-A VUS, which only the positive control is significant. Statistical significance is represented with * (the amount of * represents how relevant is the statistical difference).

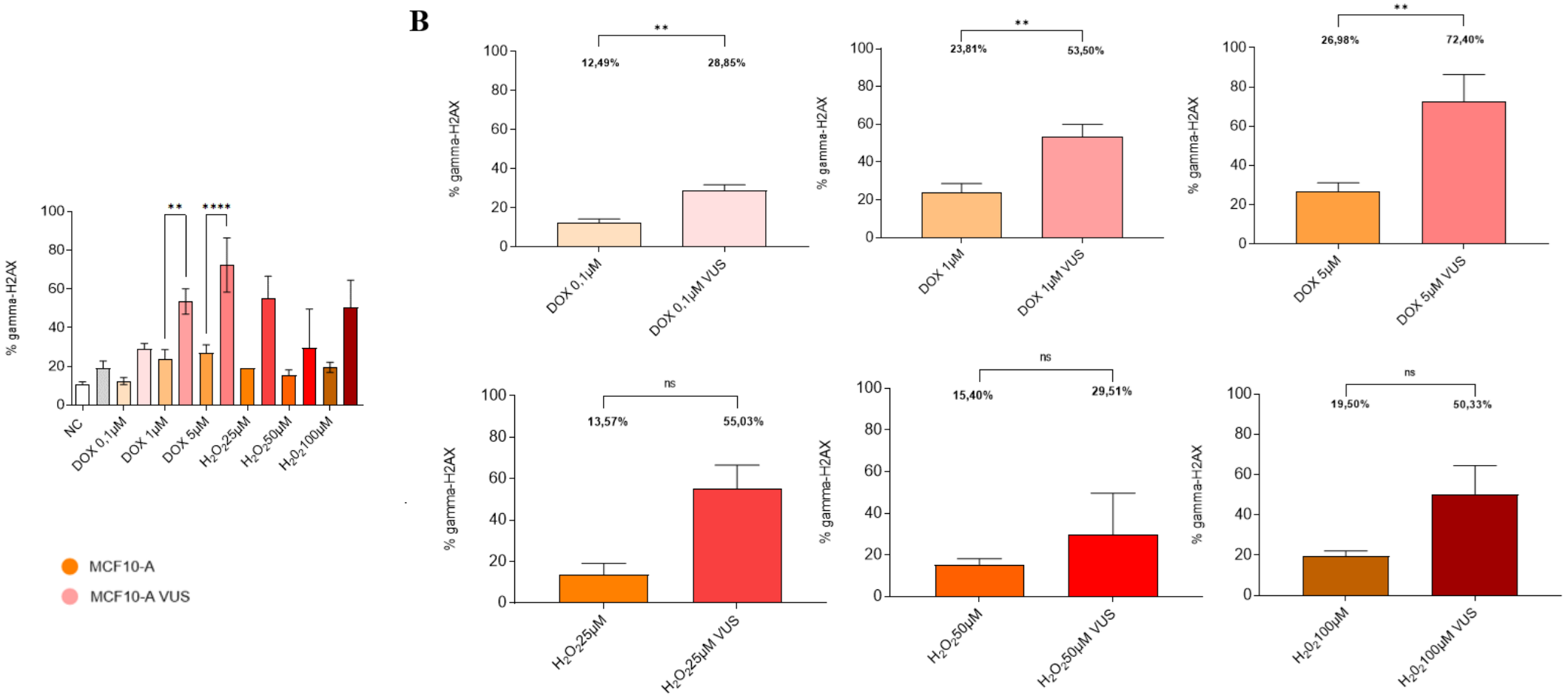

Figure 3.10 - Comparison of % of γ-H2AX in each drug exposure of MCF10-A versus MCF10-A VUS. A – Overall % of γ-H2AX in each drug. **B -** % of γ-H2AX in each drug exposure and dose. All graphs were plotted using GraphPad Prism 9 software. Mean values ± SEM are represented by the black lines (orange shades MC10-A and pink shades MCF10-A). Statistical analysis with Mann-Whitney test and a p-value < 0.05 was considered statistically significant. Only DOX doses presented statistical significance differences, where MCF10-A VUS presents higher % of γ-H2AX. Statistical significance is represented with * (the amount of * represents how relevant is the statistical difference).

3.4. Annexin V

In order to analyse if the cells had a different response to the damage induced by genotoxic agents, we performed this assay, which is a measure of apoptosis. In this assay, we measure the PS exposure at the outer part of the plasma membrane. Based on Annexin-V affinity, apoptotic cell can be distinguished from live cells; Plus, when combined with PI, the double labelling allows to further distinguish necrotic and apoptotic cells. As a positive control, we use a well-known chemotherapeutic agent apoptosis inducer, CPT 5μM.

The results were obtained from FACS Canto II cytometer where around 20000 cells were collected for each treatment. After which, they were then analysed by FlowJo™ 10 software, which gave us the percentage of necrotic (Annexin V- / PI+) and apoptotic cells (Annexin V+/ PI+) in each treatment (Figure 3.11 and Figure 3.12). Unfortunately, it was only possible to perform one independent experiment of this assay, being only possible to observe tendencies instead of statistic significances. With this in mind, in Figure 3.13 (A and B) we can observe some differences; In both cell lines, MCF10-A and MCF10-A VUS, we see a massive discrepancy between apoptosis and necrosis in DOX 1μM and DOX 5μM. Also, when putting side-by-side the cell lines (Figure 3.13 - C and D), we observe that MCF10-A has higher % of cells in necrosis than MCF10-A VUS in all drugs and different concentrations. In contrast, MCF10-A VUS has higher % of cells in the apoptotic state.

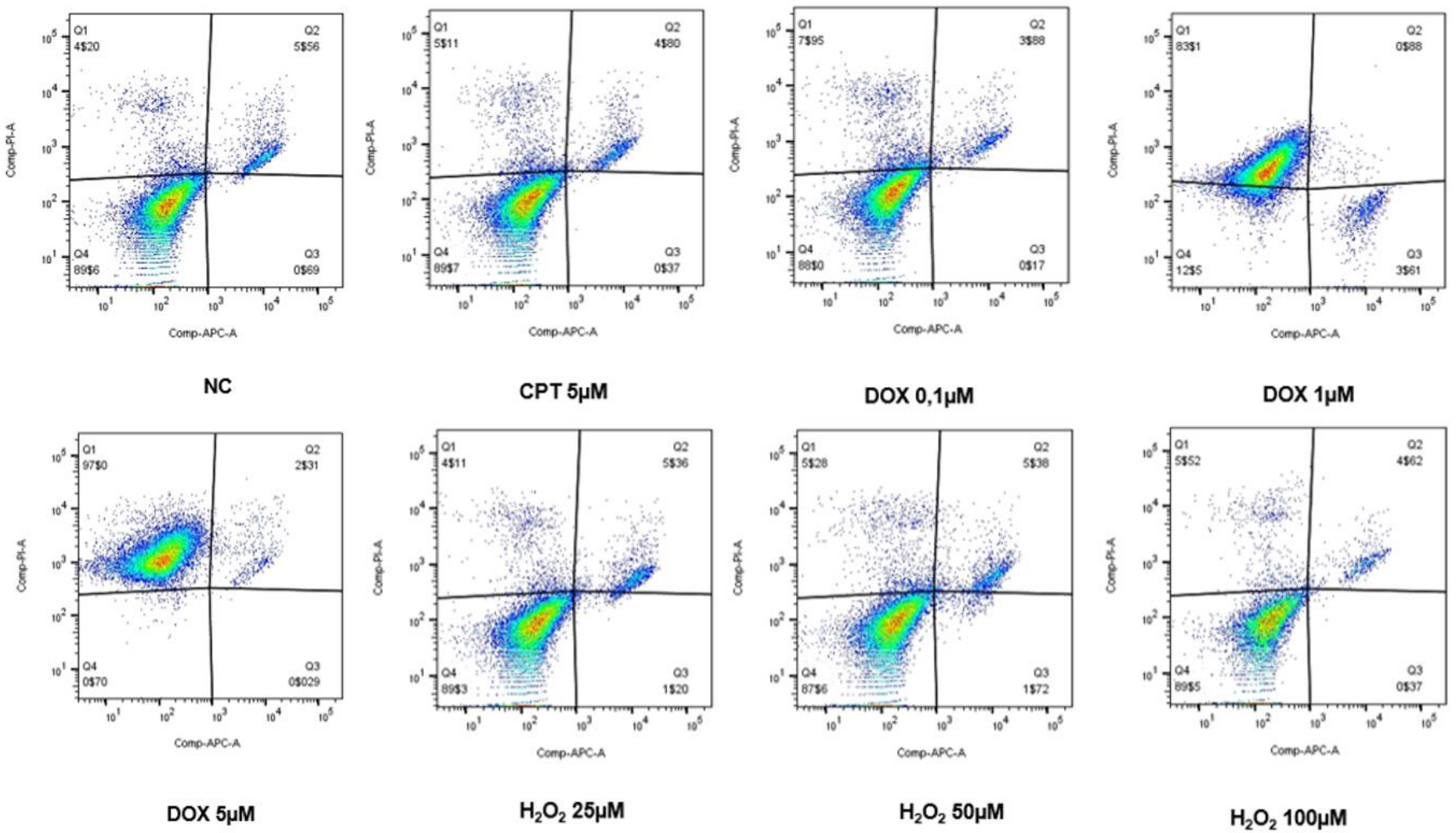

Figure 3.11 - Gating and data analysis of apoptosis and necrosis through flow cytometry in MCF10-A samples. Data analysis through FlowJo™ software. APC-A represents the staining from Annexin V, whereas PI represents live or dead cells. Legend: Q4 – Live cells (Annexin V- / PI-); Q3- Early apoptosis (Annexin V+ / PI-); Q2 – Apoptosis (Annexin V+ / PI+); Q1 – Necrosis (Annexin V- / PI+).

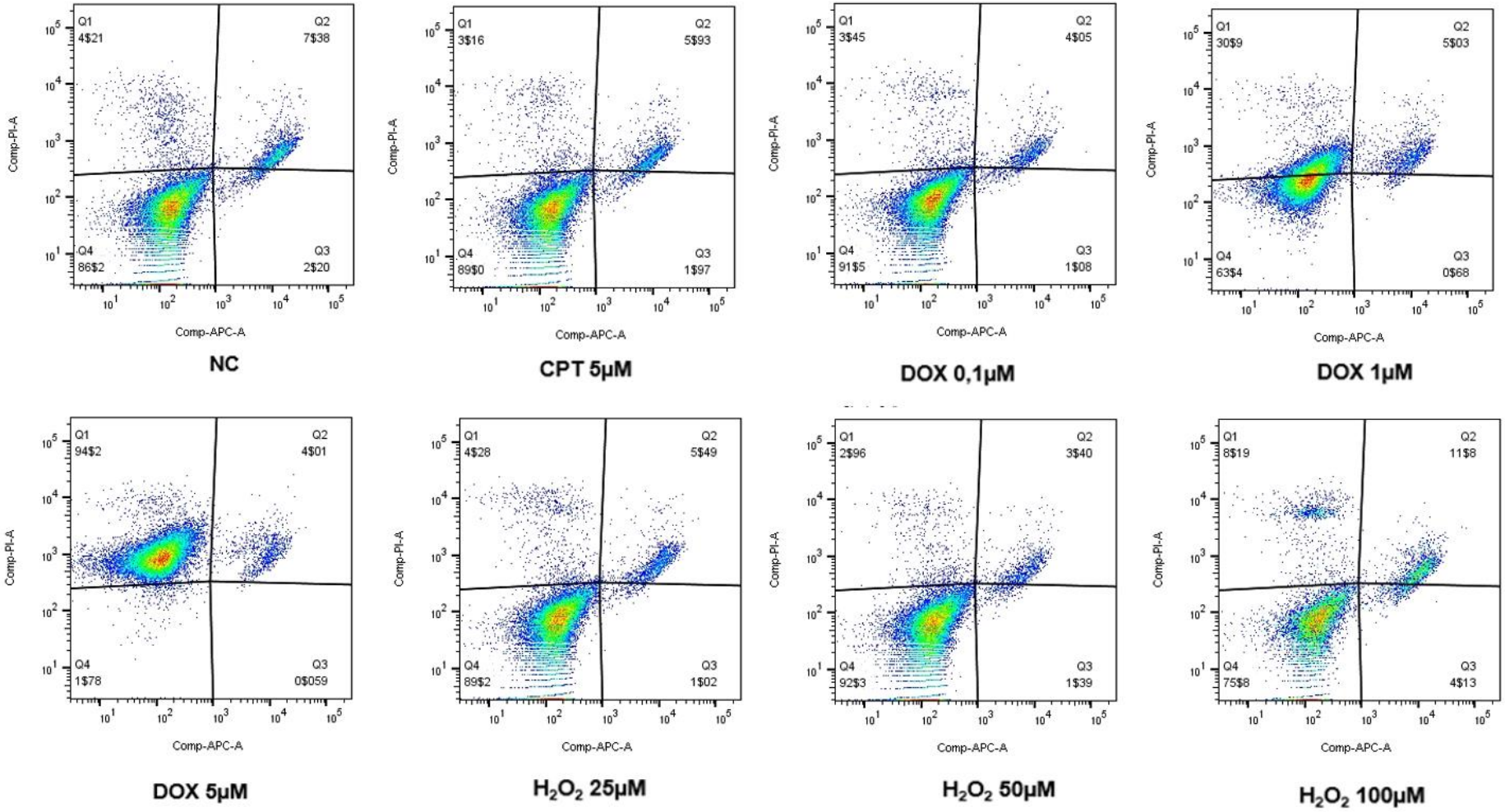

Figure 3.12 - Gating and data analysis of apoptosis and necrosis through flow cytometry in MCF10-A VUS samples. Data analysis through FlowJo™ software. APC-A represents the staining from Annexin V, whereas PI represents live or dead cells. Legend: Q4 – Live cells (Annexin V- / PI-); Q3- Early apoptosis (Annexin V+ / PI-); Q2 – Apoptosis (Annexin V+ / PI+); Q1 – Necrosis (Annexin V- / PI+).

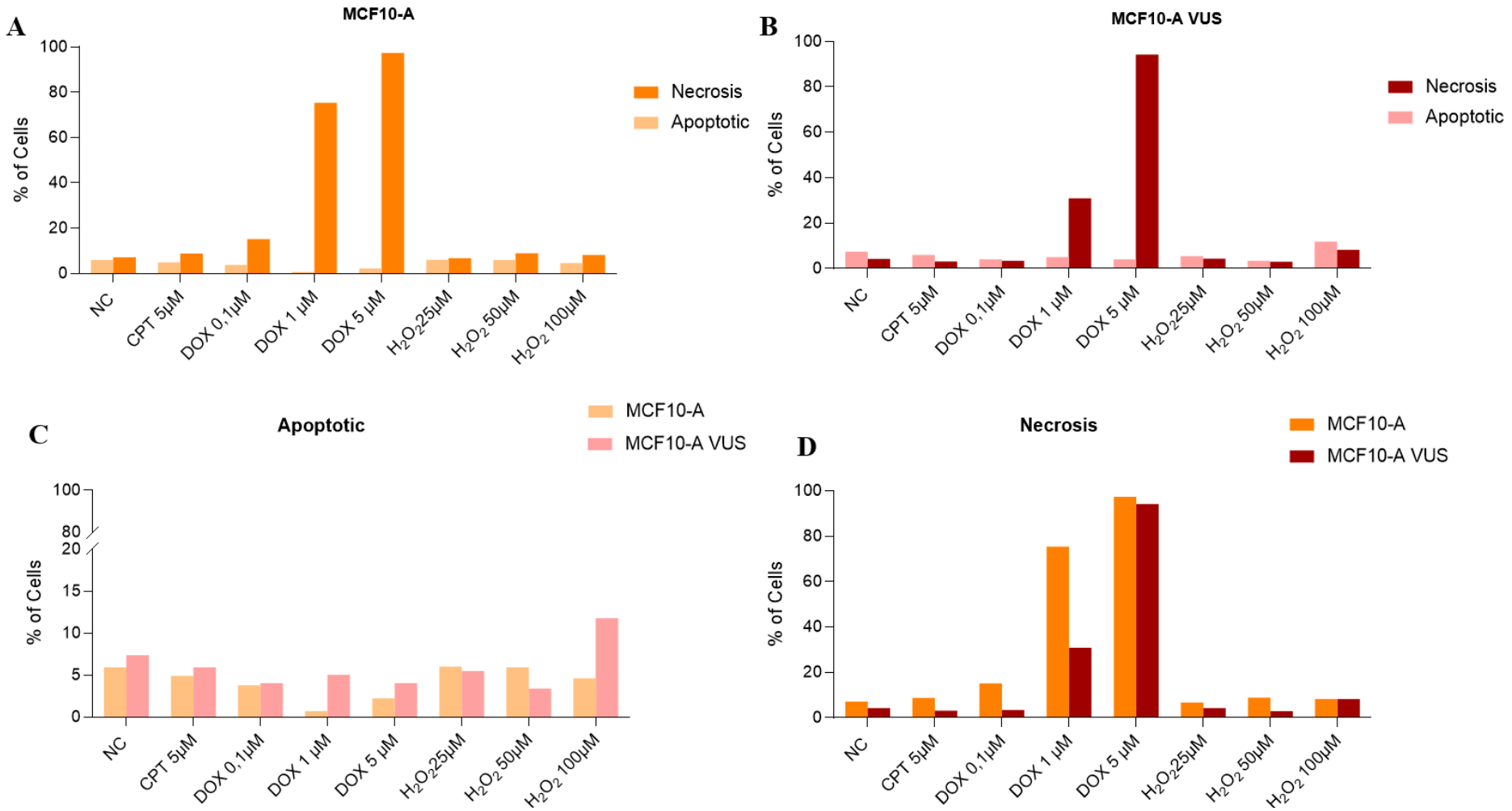

Figure 3.13 - Overall of % of apoptotic and necrotic cells in each drug exposure of MCF10-A (A) and MCF-10-A VUS (B). C – % of apoptotic cells MCF10-A versus MCF10-A VUS in each drug exposure and dose. **D -** % of necrotic cells MCF10-A versus MCF10-A VUS in each drug exposure and dose. All graphs were plotted using GraphPad Prism 9 software.

3.5. Western Blot

For a better understanding of how our VUS could affect the protein production, we performed western blot to obtain a semi-quantitative estimation: thickness of the band and intensity, corresponding to the protein expression.

To obtain a more accurate result, we did a gradient of concentration for our protein sample – 10µg, 20µg and 30µg- were the concentration of 10µg of protein had the best results. The visualization of protein bands was observed through Chemidoc™. Afterwards, we use ImageJ software to compare the density or intensity of the bands. Next, the relative expression of our protein of interest, was normalized to our protein control, β-actin. As we can see in Figure 3.14, MCF-7 has the higher expression of BRCA1 protein, while MCF10-A VUS has the lowest. Furthermore, we compared the MCF10-A VUS with MCF10-A and detect a decreased of approximately 50% (49.7%) of the *BRCA1* relative expression.

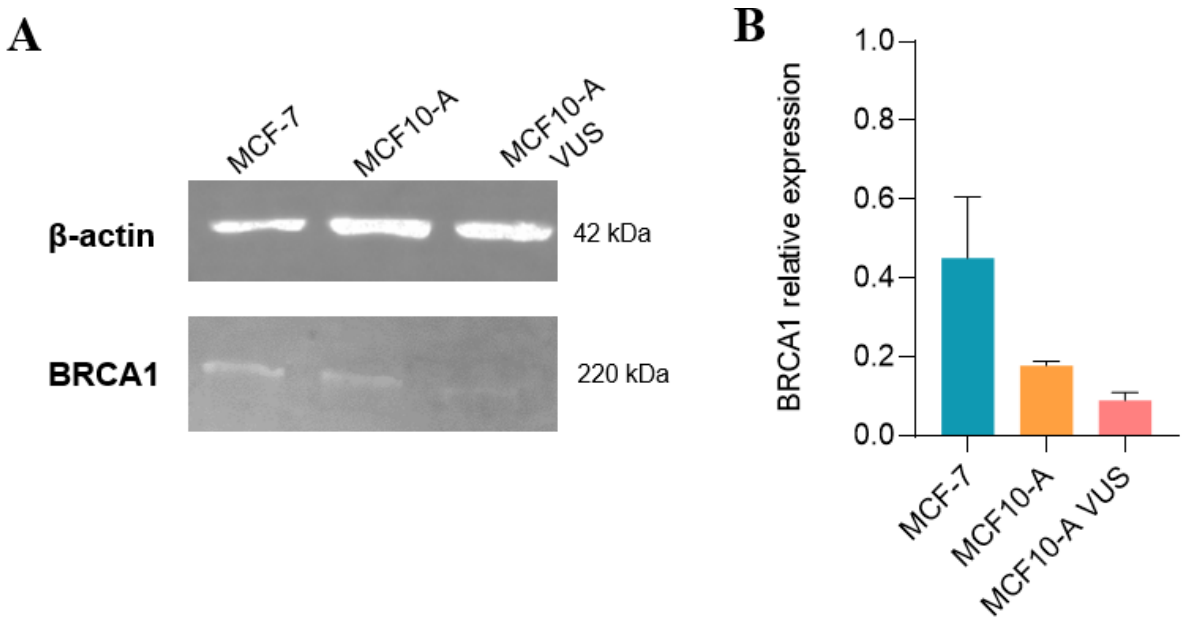

Figure 3.14- Results of Western Blot analysis for BRCA1 protein expression. A- BRCA1 protein expression in MCF-7, MCF10-A and MCF10-A with inserted VUS (n=2). β-actin, a housekeeping protein, served as loading control (n=2). **B-** Densitometric analysis performed with ImageJ. The graph was plotted as mean values ± SEM are represented by the black lines using GraphPad Prism 9 software.

4. Discussion and Proof-of-concept

Discussion

DNA molecules are highly susceptible to chemical modifications. As they are constantly under damage exposure to numerous damaging agents, it is crucial that proper repair mechanisms act effectively to maintain cellular integrity and stability. If the damage is left unrepaired or incorrect DNA damage repair and response occurs, it may enhance DNA vulnerability to damaging agents, thus increasing replication stress. DSB are extremely hazardous lesions, and the main cause of genomic instability – a key hallmark of cancer (Chatterjee e Walker, 2017; Kalimutho *et al.*, 2019). In mammalian cells, there are two main pathways to repair DSBs: HR and NHEJ (Hoeijmakers, 2001). Therefore, if these repair pathways lose their functionality, they may lead to improper DSB repair, thus leading to carcinogenesis. HR impairment has been linked to BC development, unsurprisingly, most of the genes tested in panels associated with this cancer are leading players in DSB repair (Economopoulou, Dimitriadis e Psyrri, 2015; Gorodetska, Kozeretska e Dubrovska, 2019). These gene panels are now easily sequenced due to the development of high throughput methodologies as NGS, which allows the detection of pathogenic mutations in related genes but also, multiple VUS. Nevertheless, the accurate of VUS identified remains unclear, even though several strategies exist, most only offer the theoretical effect of the variant. Hence, an essential but still not clarified question is the possible role of these gene variants and their potential effect on cancer risk, which only functional assays can answer (Calò *et al.*, 2010; Millot *et al.*, 2012).

In previous studies we found a VUS in the *BRCA1* gene in patients with no cancer, but with a high occurrence of cancer in the family history. Our variant change occurs in the residue 356 of the BRCA1 protein, whereas arginine is produced instead of a glutamine. As mentioned before, BRCA1 associates with the MRN complex of proteins; this is mediated by the RAD50 with the residues 341–748 of the BRCA1. The activity of BRCA1 and MRN complex is cell cycle dependent acting in late S and G2 phases. Furthermore, this complex may act as a sensor of DSBs, through the phosphorylation of H2AX (γ-H2AX), signalling the recruitment of the downstream DNA repair pathway, promoting HR instead of NHEJ (Christou e Kyriacou, 2012). Although it is still unclear if a missense variant, such a subtle change, can alter the function of the protein, its known that the location is key to infer the pathogenicity of a variant (Calò *et al.*, 2010; Radice *et al.*, 2011).

With this in mind, our group had already performed some functional assays on the patients' peripheral blood using γ - radiation and through genotoxic challenge with DOX. Even though with the patients' peripheral blood for these assays we had access to the whole genetic background of the patients, it is a burden and time-consuming to ask for the patients' blood. Therefore, to overcome this step, we choose to use cell lines allowing an

efficient follow-up with no sample size limitation and with the ability to replicate studies. Since no cell lines had our VUS of interest, we would have to introduce the VUS into a non-tumorigenic breast cell line (MCF10-A) since our patients do not have cancer, but also to a tumorigenic breast cell line (MCF-7) to study if the VUS can be a potential enhancer of tumour aggressiveness. This last cell line has an interesting characteristic: is hemizygous for the gene *BRCA1,* meaning that there is only one copy of the gene. Moreover, this has been associated with deficient processing of DNA damage induced by ROS (Francisco *et al.*, 2008).

We used CRISPR-Cas9 as a genome-editing tool to introduce the VUS of interest into MCF10-A and MCF-7 cell lines. Since studies with patients' blood had already been and are still being carried out by our group, we can always compare the results from the CRISPR-Cas9 cell lines with the lymphocytes from the patients, giving us a proof of concept that the edited cell line has similar results to the patients' lymphocytes (Adubeiro, R, 2018; Lança, 2019). When establishing this idea, we can take advantage of genome editing tools to confirm that not only this VUS, but many others can be studied through this more accessible methodology. Briefly, CRISPR-Cas9 is a genome-editing tool, where the sgRNA recruits the Cas 9 nuclease to a specific locus to generate a DSB. These can either be repaired by HR or NHEJ. HR is more conservative and error-free and has already been reported to work *in vitro* cell cultures, however, is dependent on a repair template (ssODN) (Inui *et al.*, 2014). To achieve the best efficiency for CRISPR-Cas9, two steps of utmost importance must be taken into consideration: the correct design of the sgRNA and of the ssODN. Using CRISPR Design Tool (CRISPOR) it was possible to preview the minimization of off-targets but also, to enhance Cas9 nuclease sensitivity and to achieve high HR efficiency (Ran *et al.*, 2013). These were already optimized in our group, as well as the expression plasmid selection (pX458) and constructions with the sgRNA (Pires, Maria J, 2019). In order to ensure the correct introduction of the sgRNA into the pX458, a double digestion with BpiI and BshTI restriction enzymes was performed, where a successful insertion will destroy the BpiI sites. As expected, clones with the insertion (sgRNA) only showed a linearized plasmid of ~8.5kb, where only BshTI (restriction site present in pX458) was able to cut. Clones without the insertion (no sgRNA) showed ~1kb and ~7.5kb fragment, where both BpiI and BshTI were able to cut (Figure 3.1).

Afterwards, we transfected the cell lines with our clones pX458 sgRNA plus ssODN using PEI as the transfection agent; the isolation and selection of these was made through flow cytometry to a 96-well plate until cells reached enough confluence to extract the DNA (Figure 3.2.). Albeit, MCF-7 has a higher transfection rate (6.26%) than MCF10-A (1.24%), the cells selected through flow cytometry did not proliferate, perhaps due to the cytotoxicity induced by PEI (Moghimi et al., 2005; Mokhtary et al., 2018). In contrast, we were able to

achieve a heterozygous clone for the VUS with the MCF10-A cell line, amongst fourteen clones, one of them appears to be for the VUS: C**A**G– FW and C**C**G – RV (Figure 3.5) despite the low transfection rate. Inserting a point mutation with CRISPR-Cas9 is much more challenging than knock-in or knock-out of an entire gene, being indeed time-consuming to achieve the specific clones. Introducing the ssODN may not be enough for the repair to occur through HR, because it only takes place during the S and G2 phases, but it may also depend on the cell type, target locus, type of repair donor and location of alteration relative to the DSB site (Ran *et al.*, 2013). With this in mind, we need to focus on how to improve the transfection efficiency not only for MCF-7 but also MCF10-A, perhaps by optimising the ratio of transfection reagent per plasmid DNA or the cell number per well when transfecting, or even using other transfection reagents available, for example lipofectamine, since these cells seem to be hard to transfect.

One step that should be optimized is the background noise observed after sequencing. This is a characteristic disadvantage of Sanger sequencing; The background noise is observed in the first peaks and towards the end of the sequencing, often in lumpy peaks, one peak being beneath another or even in two successive peaks for the same base being merged into one. (Ewing *et al.*, 1998). Despite the VUS being present in a background noise trace, we can clearly observe the peak beneath correspondent to the point mutation of interest (C**C**G – RV). Another hypothesis for the background noise is population heterogeneity This probably happened because when performing single-cell isolation, we selected two cells per well, so that the cells would grow faster. Furthermore, MCF-7 has chosen with the intent to explore the VUS as a potential enhancer of pathogenicity, but we weren't able to establish the cell line with the VUS. Nevertheless, the functional assays in MCF-7 were performed for posterior comparison against the MCF-7 VUS.

The comet assay is a simple, rapid and sensitive method for detecting low levels of DNA damage breaks in individual cells (Collins, 2004). H_2O_2 was used as a positive control because it allows the accumulation of ROS, thus leading to DNA damage mostly SSBs. As expected, all cell lines had statistical differences between the NC and the positive control H_2O_2 50µM on the %DNA tail. Nevertheless, neutral single-cell electrophoresis would be more appropriate since it only allows the detection of DSBs, removing like this the interference of the SSBs. Observing each cell line individually (Figure 3.7.), in MCF10-A we can observe statistical differences in all drugs and concentration: as we increase the dose of DOX so does the % DNA tail (DOX 0,1µM – 13.02%, DOX 1µM – 13.94% and DOX 5µM – 20.64%) resulting in a concentration effect. In MCF10-A VUS, only DOX 5µM (13.73%) and H_2O_2 50µM (22.71%) had a statistically significant difference against the NC. The tumorigenic cell line, MCF-7 had the lowest values of % DNA in tail, having only statistical significance with the positive control (6.44%). Nevertheless, when observing the DNA damage induced treatment-by-treatment

amongst the MCF10-A and the VUS cells line the situation changes: all groups were statistically significant. The non-tumorigenic cell line has a higher sensitivity, which means more DNA damage. Most importantly, the MCF10-A VUS has lower % DNA tail than MCF10-A (Figure 3.8). With this in mind, it is possible that the cells with impaired HR and with excessive genome damage, could use other pathways, more likely related to cell death to stop proliferating the damaged cells, thus eliminating the damage. There is also the possibility that the VUS may be benign. As mentioned before, these results can be compared with the functional assays performed with the patients' lymphocytes; the VUS-carriers seem to have similar or lower % DNA in tail, these differences can be due to intra and/or inter-individuality and not directly to the variant (Lança, 2019). Nevertheless, more assays still need to be performed to have a more concrete idea, such as apoptosis and necrosis assays. We could also understand how the cells repair the damage-induced, by inducing the damage and then allowing the cells to repair it about 30 min as we did with the ɣ-H2AX (Collins, 2004).

ɣ-H2AX assay is more sensitive and specific for DNA DSBs. Therefore, H_2O_2 50μM would not be the most appropriate candidate for positive control, since it creates DNA damage through the formation of ROS. So, DOX 5μM was chosen to be our positive control instead, since it induces DSBs. Usually, this methodology is performed through fluorescent microscopy, however by flow cytometry it allows a more quick and sensitive quantification of the DNA damage (Huang e Darzynkiewicz, 2006; Kopp, Khoury e Audebert, 2019). In addition, our cell lines grows preferentially in clusters, becoming difficult to observe the green foci of the phosphorylated H2AX (ɣ-H2AX) through fluorescent microscopy. We have also introduced some more H_2O_2 concentrations to build a gradient. Overall, DOX 1μM and 5μM had statistically significant % ɣ-H2AX when compared to the NC, with exception to MCF10-A VUS were only DOX 5μM (72.40%) showed significance (Figure 3.9). In this technique, MCF-7 seems to have increased sensitivity to doxorubicin: the % ɣ-H2AX is much higher when compared to % DNA in tail under all treatments, but especially DOX 1μM (94.55%) and DOX 5μM (99.50%), nonetheless the NC has also increased (51.75%). The non-tumorigenic MCF10-A cells DOX 5μM had a higher frequency of ɣ-H2AX (26.98%), followed by DOX 1μM (23.81%). For MCF10-A VUS the %ɣ-H2AX increases with the DOX concentration: DOX 0,1μM – 28.85%, DOX 1μM – 53.50% and DOX 5μM – 72.40%. As expected H_2O_2, has no statistical significance in all cell lines, since H_2O_2 creates DNA damage through the formation of ROS, resulting essentially in SSB. Afterwards, we compared the DNA damage induced treatment-by-treatment amongst the cells; MCF10-A and MCF10-A VUS only DOX concentrations have significance differences (Figure 3.10). This methodology has also been tested with the patients' blood and there seem to be no statistical differences neither between controls, nor between doxorubicin concentrations and the negative control,

except for DOX 5μM, which shows a highly increased %ɣ-H2AX, both in the control patients and VUS-carriers (Lança, 2019). Once again, these results were concordant with those obtained with MCF10-A VUS. Possibly, we are observing the DOX concentration effect, instead of the variant.

Other approaches could be performed to better understand the role of the VUS. Concerning that many times the chemotherapeutic treatments combined differently several, could be considered to combine DOX with, for example, Poly-ADP-ribose polymerase inhibitors (PARPi). This chemotherapeutic drug leads to a faulty repair of SSBs, without affecting DSB repair. If SSBs do not become repaired, these stall and collapse replication forks resulting in DSBs that are usually repaired through HR. Thus, if the cell has a deficient HR, like *BRCA* mutations, the DSBs are repaired inaccurately or through NHEJ leading to DNA damage accumulation and tumour cell death. The advantage about PARPi is that it is not toxic to healthy cells but highly cytotoxic to HR impaired cells with *BRCA* deficiencies (Franzese *et al.*, 2019; Jackson e Bartek, 2009). This approached was already tested in previous studies by our group and the results pointed-out to the evidence that PARPi is indeed non-toxic to MCF10-A, no statistically significant difference was found in any of the used concentrations for the % ɣ-H2AX (Pires, Maria J, 2019). Other alternative, could be to allow the cells repair for a longer period of time, to see if the DNA damage repair pathway is indeed compromised. Nevertheless, other chemotherapeutic might be considered as an alternative, such as cisplatin or docetaxel to assess *BRCA1* in HR pathway (Postel-Vinay *et al.*, 2012).

To better understand if the cells are using other pathways, such as apoptosis, we performed Annexin V assay. The different morphological features of phosphatidyl serine in the cell membrane allows to measure the apoptosis stages through the conjugation of PI and Annexin V: viable (Annexin V - / PI -), early apoptotic (Annexin V+ / PI -), later apoptotic (Annexin V+ /PI +) and necrotic (Annexin V- /PI +). This methodology when combined with flow cytometry, distinguishes apoptosis and necrosis at the single cell level (Pietkiewicz, Schmidt e Lavrik, 2015). Unfortunately, due to unforeseen problems in the laboratory we could only perform one independent experiment, thus we will observe tendencies instead of statistic significances. With this is mind, the % of cells in each stage were assessed only in the MCF10-A and MCF10-A VUS cell lines. For our positive control, we choose a well-known apoptosis inducer drug, CPT. Although we cannot assess real percentages, we can observe a massive discrepancy between apoptosis and necrosis in particular with DOX 1μM and DOX 5μM in both cell lines. Lastly, and comparing side-by-side the cell lines (Figure 3.13 - C and D), we observe that MCF10-A has higher % of cells in necrosis than MCF10-A VUS in all drugs and different concentrations. In contrast, MCF10-A VUS has higher % of cells in the apoptotic state. The principal damage of DOX is the induction of DSB, nonetheless it can also interfere

with the integrity of the membrane due the formation of ROS, increasing lipid peroxidation, but also, other mechanisms due to its promiscuity of action. Nevertheless, more assays still need to be performed to have a more concrete idea, such as Caspases 3, 7, and 9 assays or the Tunnel assay, enabling the comparison of the results with the ones obtained with the patients' blood, which were already done (Lança, 2019).

Even though we cannot infer if the VUS can or cannot interfere directly with the protein function, we can assess the relative expression level of BRCA1 in the cell lines through Western Blot. Through the thickness of the band and intensity through ImageJ software, we could observe that MCF-7 has the higher expression of BRCA1 protein, while MCF10-A VUS has the lowest. Furthermore, we compared the MCF10-A VUS with MCF10-A and detect a decreased of approximately 50% (49.7%) of the BRCA1 expression. Nevertheless, the results obtained for the tumorigenic cell line disagree with the literature (Francisco *et al.*, 2008), as MCF10-A should have the higher expression of BRCA1 protein. As stated before, MCF-7 is hemizygous for *BRCA1*, consequently there is an inherent impaired expression of the protein, enhancing the need to repeat this assay. Furthermore, as an alternative to Western Blot we can perform qRT-PCR, which is more sensitive, specific, and accurate in the relative quantification of the expression of proteins. Regarding the decreased expression of BRCA1 in MF10-A VUS cells, the results are too preliminary to infer the direct correlation to the DNA damage.

If we take into consideration our results and those from previous studies with the patients' blood, we can risk classifying our VUS as benign. More interestingly, we can see a protective behaviour; thus if our VUS was only benign we can expect to observe no differences between MCF10-A and MCF10-A VUS. Nonetheless, we observe not only less DNA damage in the comet assay, but also, less necrosis when the VUS is present. Despite the results being preliminary, they are in agreement with meta-analysis studies; not only the VUS is benign but also it has a lower risk of BC associated with this VUS-carriers demonstrating a protective behaviour (Brignoni *et al.*, 2020; Xu *et al.*, 2018). Therefore, more functional assays need to be performed to better understand the role of our VUS in the DNA damage repair pathway.

Furthermore, we can conclude that the use of CRISPR-Cas 9 to edit cell lines with the VUS of interest, is a reliable methodology for the functional study of variants, thus assess of the risk disease. Through comparison, our results are in concordance with the results obtain with the patient's blood (Lança, 2019). Nevertheless, our model presents one limitation - the absence of the patients' genetic background. In order to overcome this limitation, we are also establishing immortalised lymphoblastoid cell lines, using the patient's lymphocytes.

The identification and classification of genetic variant associations with clinical phenotypes is an ambitious goal in medical research. These kind of projects are of highest importance, since they associate basic and clinical research. It is crucial to identify the pathogenicity status of a large amount of VUS, that have already been identified in the population - in BC, but also in other types of cancer - in order to provide a better prognosis and if needed treatment for at-risk family members.

5. References

References

ADUBEIRO, R - Functional Characterization of Variants of Unknown Significance in Familial Breast Cancer

AMIR, Eitan *et al.* - Targeting DNA repair in breast cancer: A clinical and translational update. Cancer Treatment Reviews. . ISSN 03057372. 36:7 (2010) 557–565. doi: 10.1016/j.ctrv.2010.03.006.

APARICIO, Tomas; BAER, Richard; GAUTIER, Jean - DNA double-strand break repair pathway choice and cancer. DNA repair. . ISSN 1568-7864. 19:2014) 169–175. doi: 10.1016/j.dnarep.2014.03.014.

AUGUSTO, Bianca M. *et al.* - From the laboratory to the clinic: sharing BRCA VUS reclassification tools with practicing genetics professionals. Journal of Community Genetics. . ISSN 1868-6001. 9:3 (2018) 209–215. doi: 10.1007/s12687-017-0343-3.

BOLDERSON, E. *et al.* - Recent Advances in Cancer Therapy Targeting Proteins Involved in DNA Double-Strand Break Repair. Clinical Cancer Research. . ISSN 1078-0432, 1557-3265. 15:20 (2009) 6314–6320. doi: 10.1158/1078-0432.CCR-09-0096.

BRADFORD, M. M. - A rapid and sensitive method for the quantitation of microgram quantities of protein utilizing the principle of protein-dye binding. Analytical Biochemistry. . ISSN 0003-2697. 72:1976) 248–254. doi: 10.1006/abio.1976.9999.

BRAY, Freddie *et al.* - Global cancer statistics 2018: GLOBOCAN estimates of incidence and mortality worldwide for 36 cancers in 185 countries. CA: A Cancer Journal for Clinicians. . ISSN 1542-4863. 68:6 (2018) 394–424. doi: 10.3322/caac.21492.

BRIGNONI, Lucía *et al.* - Genomic Diversity in Sporadic Breast Cancer in a Latin American Population. Genes. . ISSN 2073-4425. 11:11 (2020) 1272. doi: 10.3390/genes11111272.

CALÒ, Valentina *et al.* - The Clinical Significance of Unknown Sequence Variants in BRCA Genes. Cancers. . ISSN 2072-6694. 2:3 (2010) 1644–1660. doi: 10.3390/cancers2031644.

CHAPMAN, J. Ross; TAYLOR, Martin R. G.; BOULTON, Simon J. - Playing the End Game: DNA Double-Strand Break Repair Pathway Choice. Molecular Cell. . ISSN 10972765. 47:4 (2012) 497–510. doi: 10.1016/j.molcel.2012.07.029.

CHATTERJEE, Nimrat; WALKER, Graham C. - Mechanisms of DNA damage, repair, and mutagenesis: DNA Damage and Repair. Environmental and Molecular Mutagenesis. . ISSN 08936692. 58:5 (2017) 235–263. doi: 10.1002/em.22087.

CHERN, Jing-Yi *et al.* - The influence of BRCA variants of unknown significance on cancer risk management decision-making. Journal of Gynecologic Oncology. . ISSN 2005-0380. 30:4 (2019). doi: 10.3802/jgo.2019.30.e60.

CHRISTOU, Charita M.; KYRIACOU, Kyriacos - BRCA1 and Its Network of Interacting Partners. Biology. . ISSN 2079-7737. 2:1 (2012) 40–63. doi: 10.3390/biology2010040.

ClinVar - NCBI - [Em linha], atual. 2020. [Consult. 19 dez. 2020]. Disponível em WWW:<URL:https://www.ncbi.nlm.nih.gov/clinvar/variation/41803/>.

COLLINS, Andrew R. - The Comet Assay for DNA Damage and Repair: Principles, Applications, and Limitations. Molecular Biotechnology. . ISSN 1073-6085. 26:3 (2004) 249–261. doi: 10.1385/MB:26:3:249.

ECONOMOPOULOU, P.; DIMITRIADIS, G.; PSYRRI, A. - Beyond BRCA: new hereditary breast cancer susceptibility genes. Cancer Treatment Reviews. . ISSN 1532-1967. 41:1 (2015) 1–8. doi: 10.1016/j.ctrv.2014.10.008.

ELMORE, Susan - Apoptosis: A Review of Programmed Cell Death. Toxicologic pathology. . ISSN 0192-6233. 35:4 (2007) 495–516. doi: 10.1080/01926230701320337.

EWING, Brent *et al.* - Base-Calling of Automated Sequencer Traces Using *Phred.* I. Accuracy Assessment. Genome Research. . ISSN 1088-9051, 1549-5469. 8:3 (1998) 175–185. doi: 10.1101/gr.8.3.175.

FENG, Yixiao *et al.* - Breast cancer development and progression: Risk factors, cancer stem cells, signaling pathways, genomics, and molecular pathogenesis. Genes & Diseases. . ISSN 2352-3042. 5:2 (2018) 77–106. doi: 10.1016/j.gendis.2018.05.001.

FIRSANOV, Denis *et al.* - Rapid Detection of γ-H2AX by Flow Cytometry in Cultured Mammalian Cells. Em DIDENKO, VLADIMIR V. (Ed.) - Fast Detection of DNA DamageMethods in Molecular Biology. [Em linha]. New York, NY : Springer New York, 2017 [Consult. 10 nov. 2020]. Disponível em WWW:<URL:http://link.springer.com/10.1007/978-1-4939-7187-9_11>. ISBN 978-1-4939-7185-5v. 1644. p. 129–138.

FRANCISCO, Dave C. *et al.* - Induction and processing of complex DNA damage in human breast cancer cells MCF-7 and nonmalignant MCF-10A cells. Free Radical Biology and Medicine. . ISSN 08915849. 44:4 (2008) 558–569. doi: 10.1016/j.freeradbiomed.2007.10.045.

FRANZESE, Elisena *et al.* - PARP inhibitors in ovarian cancer. Cancer Treatment Reviews. . ISSN 0305-7372, 1532-1967. 73:2019) 1–9. doi: 10.1016/j.ctrv.2018.12.002.

GEORGOULIS, Anastasios *et al.* - Genome Instability and γH2AX. International Journal of Molecular Sciences. . ISSN 1422-0067. 18:9 (2017) 1979. doi: 10.3390/ijms18091979.

GLOBOCAN 2020 - Cancer today [Em linha] [Consult. 10 fev. 2021]. Disponível em WWW:<URL:http://gco.iarc.fr/today/home>.

GORODETSKA, Ielizaveta; KOZERETSKA, Iryna; DUBROVSKA, Anna - BRCA Genes: The Role in Genome Stability, Cancer Stemness and Therapy Resistance. Journal of Cancer. . ISSN 1837-9664. 10:9 (2019) 2109–2127. doi: 10.7150/jca.30410.

HANAHAN, Douglas; WEINBERG, Robert A. - Hallmarks of Cancer: The Next Generation. Cell. . ISSN 0092-8674, 1097-4172. 144:5 (2011) 646–674. doi: 10.1016/j.cell.2011.02.013.

HARBECK, Nadia *et al.* - Breast cancer. Nature Reviews Disease Primers. . ISSN 2056-676X. 5:1 (2019) 66. doi: 10.1038/s41572-019-0111-2.

HOEIJMAKERS, Jan H. J. - Genome maintenance mechanisms for preventing cancer. Nature. . ISSN 0028-0836, 1476-4687. 411:6835 (2001) 366–374. doi: 10.1038/35077232.

HOEIJMAKERS, Jan H. J. - DNA Damage, Aging, and Cancer. New England Journal of Medicine. . ISSN 0028-4793, 1533-4406. 361:15 (2009) 1475–1485. doi: 10.1056/NEJMra0804615.

HUANG, Xuan; DARZYNKIEWICZ, Zbigniew - Cytometric Assessment of Histone H2AX Phosphorylation. Em HENDERSON, DARYL S. (Ed.) - DNA Repair ProtocolsMethods in Molecular Biology. [Em linha]. Totowa, NJ : Humana Press, 2006 [Consult. 4 nov. 2020]. Disponível em WWW:<URL:http://link.springer.com/10.1385/1-59259-973-7:073>. ISBN 978-1-58829-513-2v. 314. p. 73–80.

INUI, Masafumi *et al.* - Rapid generation of mouse models with defined point mutations by the CRISPR/Cas9 system. Scientific Reports. . ISSN 2045-2322. 4:1 (2014) 5396. doi: 10.1038/srep05396.

JACKSON, Stephen P.; BARTEK, Jiri - The DNA-damage response in human biology and disease. Nature. . ISSN 0028-0836, 1476-4687. 461:7267 (2009) 1071–1078. doi: 10.1038/nature08467.

JOHNSON-ARBOR, Kelly; DUBEY, Ramin - Doxorubicin. Em StatPearls [Em linha]. Treasure Island (FL) : StatPearls Publishing, 2020 [Consult. 19 dez. 2020]. Disponível em WWW:<URL:http://www.ncbi.nlm.nih.gov/books/NBK459232/>.

KALIMUTHO, Murugan *et al.* - Patterns of Genomic Instability in Breast Cancer. Trends in Pharmacological Sciences. . ISSN 01656147. 40:3 (2019) 198–211. doi: 10.1016/j.tips.2019.01.005.

KOPP, B.; KHOURY, L.; AUDEBERT, Marc - Validation of the γH2AX biomarker for genotoxicity assessment: a review. Archives of Toxicology. . ISSN 1432-0738. 93:8 (2019) 2103–2114. doi: 10.1007/s00204-019-02511-9.

KUMARAVEL, T. S. *et al.* - Comet Assay measurements: a perspective. Cell Biology and Toxicology. . ISSN 0742-2091, 1573-6822. 25:1 (2009) 53–64. doi: 10.1007/s10565-007-9043-9.

LANÇA, Miguel Filipe Cecília - Functional studies of genetic variants of unknown significance

LERNER-ELLIS, Jordan *et al.* - Genetic risk assessment and prevention: the role of genetic testing panels in breast cancer. Expert Review of Anticancer Therapy. . ISSN 1473-7140, 1744-8328. 15:11 (2015) 1315–1326. doi: 10.1586/14737140.2015.1090879.

LORD, Christopher J.; ASHWORTH, Alan - BRCAness revisited. Nature Reviews Cancer. . ISSN 1474-175X, 1474-1768. 16:2 (2016) 110–120. doi: 10.1038/nrc.2015.21.

MA, Ning *et al.* - Determining the Pathogenicity of a Genomic Variant of Uncertain Significance Using CRISPR/Cas9 and Human-Induced Pluripotent Stem Cells. Circulation. . ISSN 0009-7322, 1524-4539. 138:23 (2018) 2666–2681. doi: 10.1161/CIRCULATIONAHA.117.032273.

MAHMOOD, Tahrin; YANG, Ping-Chang - Western Blot: Technique, Theory, and Trouble Shooting. North American Journal of Medical Sciences. . ISSN 2250-1541. 4:9 (2012) 429–434. doi: 10.4103/1947-2714.100998.

MEREDITH, Ann-Marie; DASS, Crispin R. - Increasing role of the cancer chemotherapeutic doxorubicin in cellular metabolism. Journal of Pharmacy and Pharmacology. . ISSN 2042-7158. 68:6 (2016) 729–741. doi: https://doi.org/10.1111/jphp.12539.

MILLOT, Gaël A. *et al.* - A guide for functional analysis of *BRCA1* variants of uncertain significance. Human Mutation. . ISSN 10597794. 33:11 (2012) 1526–1537. doi: 10.1002/humu.22150.

MISHRA, Manish; TIWARI, Shuchita; GOMES, Aldrin V. - Protein purification and analysis: next generation Western blotting techniques. Expert review of proteomics. . ISSN 1478-9450. 14:11 (2017) 1037–1053. doi: 10.1080/14789450.2017.1388167.

NANDHAKUMAR, S. *et al.* - Evaluation of DNA damage using single-cell gel electrophoresis (Comet Assay). Journal of Pharmacology and Pharmacotherapeutics. . ISSN 0976-500X. 2:2 (2011) 107. doi: 10.4103/0976-500X.81903.

OLIVE, Peggy L.; BANÁTH, Judit P. - The comet assay: a method to measure DNA damage in individual cells. Nature Protocols. . ISSN 1754-2189, 1750-2799. 1:1 (2006) 23–29. doi: 10.1038/nprot.2006.5.

OUCHI, Toru - BRCA1 phosphorylation: Biological consequences. Cancer Biology & Therapy. . ISSN 1538-4047, 1555-8576. 5:5 (2006) 470–475. doi: 10.4161/cbt.5.5.2845.

PATHANIA, Shailja *et al.* - BRCA1 haploinsufficiency for replication stress suppression in primary cells. Nature Communications. . ISSN 2041-1723. 5:1 (2014) 5496. doi: 10.1038/ncomms6496.

PIETKIEWICZ, Sabine; SCHMIDT, Jörn H.; LAVRIK, Inna N. - Quantification of apoptosis and necroptosis at the single cell level by a combination of Imaging Flow Cytometry with classical Annexin V/propidium iodide staining. Applications in Imaging Flow Cytometry. Journal of Immunological Methods. . ISSN 0022-1759. 423:2015) 99–103. doi: 10.1016/j.jim.2015.04.025.

PIRES, MARIA J - Genome Editing Toll for Functional Characterization of Variants of Unknown Significance (VUS). [S.l.] : NMS/UNL, 2019

PolyPhen 2 - [Em linha], atual. 2020. [Consult. 19 dez. 2020]. Disponível em WWW:<URL:http://genetics.bwh.harvard.edu/ggi/pph2/59f28ff026c4ce1c7b1aa71d1a213728d6060666/5961431.html>.

POSTEL-VINAY, Sophie *et al.* - The potential of exploiting DNA-repair defects for optimizing lung cancer treatment. Nature Reviews Clinical Oncology. . ISSN 1759-4782. 9:3 (2012) 144–155. doi: 10.1038/nrclinonc.2012.3.

PRAKASH, Rohit *et al.* - Homologous Recombination and Human Health: The Roles of BRCA1, BRCA2, and Associated Proteins. Cold Spring Harbor Perspectives in Biology. . ISSN 1943-0264. 7:4 (2015) a016600. doi: 10.1101/cshperspect.a016600.

RADICE, P. *et al.* - Unclassified variants in BRCA genes: guidelines for interpretation. Annals of Oncology. . ISSN 0923-7534, 1569-8041. 22:2011) i18–i23. doi: 10.1093/annonc/mdq661.

RAN, F. Ann *et al.* - Genome engineering using the CRISPR-Cas9 system. Nature Protocols. . ISSN 1754-2189, 1750-2799. 8:11 (2013) 2281–2308. doi: 10.1038/nprot.2013.143.

RIEGER, Aja M. *et al.* - Modified Annexin V/Propidium Iodide Apoptosis Assay For Accurate Assessment of Cell Death. Journal of Visualized Experiments : JoVE. . ISSN 1940-087X. 50 (2011). doi: 10.3791/2597.

ROUSSET-JABLONSKI, Christine; GOMPEL, Anne - Screening for familial cancer risk: Focus on breast cancer. Maturitas. . ISSN 03785122. 105:2017) 69–77. doi: 10.1016/j.maturitas.2017.08.004.

ROY, Rohini; CHUN, Jarin; POWELL, Simon N. - BRCA1 and BRCA2: different roles in a common pathway of genome protection. Nature Reviews Cancer. . ISSN 1474-175X, 1474-1768. 12:1 (2012) 68–78. doi: 10.1038/nrc3181.

SANTOS, Catarina *et al.* - Pathogenicity Evaluation of BRCA1 and BRCA2 Unclassified Variants Identified in Portuguese Breast/Ovarian Cancer Families. The Journal of Molecular Diagnostics. . ISSN 15251578. 16:3 (2014) 324–334. doi: 10.1016/j.jmoldx.2014.01.005.

SHARMA, Babita *et al.* - BRCA1 mutation spectrum, functions, and therapeutic strategies: The story so far. Current Problems in Cancer. . ISSN 01470272. 42:2 (2018) 189–207. doi: 10.1016/j.currproblcancer.2018.01.001.

SHIBATA, A.; JEGGO, P. A. - DNA Double-strand Break Repair in a Cellular Context. Advances in Clinical Radiobiology (Part 2). Clinical Oncology. . ISSN 0936-6555. 26:5 (2014) 243–249. doi: 10.1016/j.clon.2014.02.004.

SHIOVITZ, S.; KORDE, L. A. - Genetics of breast cancer: a topic in evolution. Annals of Oncology. . ISSN 09237534. 26:7 (2015) 1291–1299. doi: 10.1093/annonc/mdv022.

SHIRTS, Brian H.; PRITCHARD, Colin C.; WALSH, Tom - Family-Specific Variants and the Limits of Human Genetics. Trends in Molecular Medicine. . ISSN 14714914. 22:11 (2016) 925–934. doi: 10.1016/j.molmed.2016.09.007.

SINGH, Narendra P. *et al.* - A simple technique for quantitation of low levels of DNA damage in individual cells. Experimental Cell Research. . ISSN 0014-4827. 175:1 (1988) 184–191. doi: 10.1016/0014-4827(88)90265-0.

TRAM, Eric; SAVAS, Sevtap; OZCELIK, Hilmi - Missense Variants of Uncertain Significance (VUS) Altering the Phosphorylation Patterns of BRCA1 and BRCA2. PLoS ONE. . ISSN 1932-6203. 8:5 (2013) e62468. doi: 10.1371/journal.pone.0062468.

WELSH, Jessemae L. *et al.* - Clinical Decision-Making in Patients with Variant of Uncertain Significance in BRCA1 or BRCA2 Genes. Annals of Surgical Oncology. . ISSN 1068-9265, 1534-4681. 24:10 (2017) 3067–3072. doi: 10.1245/s10434-017-5959-3.

WINTERS, Stella *et al.* - Breast Cancer Epidemiology, Prevention, and Screening. Em Progress in Molecular Biology and Translational Science [Em linha]. [S.l.] : Elsevier, 2017 [Consult. 9 jun. 2020]. Disponível em WWW:<URL:https://linkinghub.elsevier.com/retrieve/pii/S1877117317301126>. ISBN 978-0-12-812772-8v. 151. p. 1–32.

WORLD HEALTH ORGANIZATION - Cancer [Em linha] [Consult. 1 jun. 2020]. Disponível em WWW:<URL:https://www.who.int/news-room/fact-sheets/detail/cancer>.

XU, Gui-Ping *et al.* - The association between BRCA1 gene polymorphism and cancer risk: a meta-analysis. Oncotarget. . ISSN 1949-2553. 9:9 (2018) 8681–8694. doi: 10.18632/oncotarget.24064.

YARDEN, R. I. - BRCA1 at the crossroad of multiple cellular pathways: approaches for therapeutic interventions. Molecular Cancer Therapeutics. . ISSN 1535-7163, 1538-8514. 5:6 (2006) 1396–1404. doi: 10.1158/1535-7163.MCT-05-0471.

YOON, Kyong-Ah *et al.* - Clinically Significant Unclassified Variants in BRCA1 and BRCA2 Genes among Korean Breast Cancer Patients. Cancer Research and Treatment. . ISSN 1598-2998, 2005-9256. 49:3 (2017) 627–634. doi: 10.4143/crt.2016.292.

ZHAN, Tianzuo *et al.* - CRISPR/Cas9 for cancer research and therapy. Seminars in Cancer Biology. . ISSN 1044579X. 55:2019) 106–119. doi: 10.1016/j.semcancer.2018.04.001.

ZHANG, F.; WEN, Y.; GUO, X. - CRISPR/Cas9 for genome editing: progress, implications and challenges. Human Molecular Genetics. . ISSN 0964-6906, 1460-2083. 23:R1 (2014) R40–R46. doi: 10.1093/hmg/ddu125.

6. Annexes

Annex 1

Figure 6.1 - Expression plasmid pSpCas9(BB)-2A-GFP (pX458). Adapted from Addgene.

Annex 2

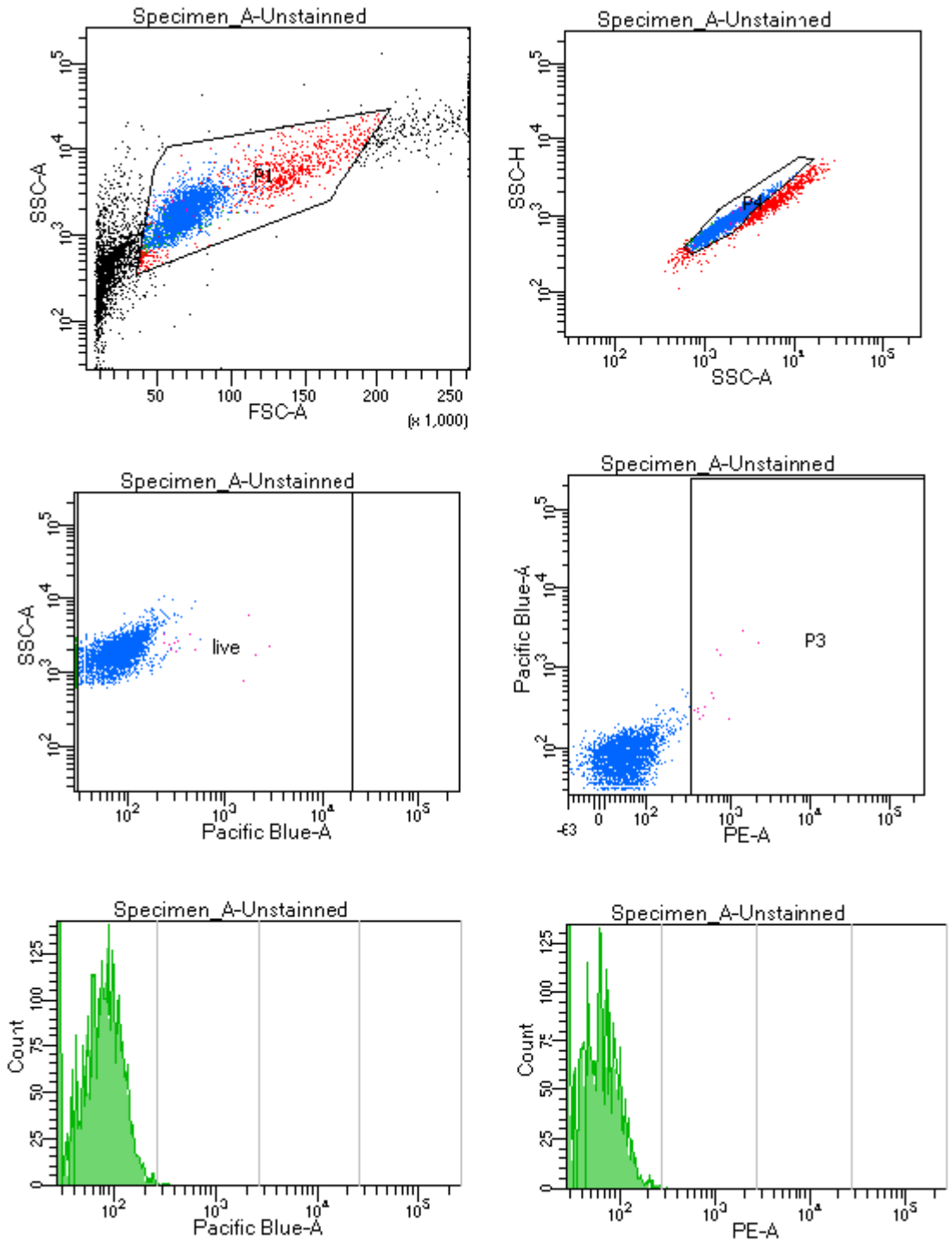

Figure 6.3 – Example of gating of γ-H2AX through flow cytometry. Gating of the unstained in flow cytometry. Pacific blue represents the staining from the LIVE/DEAD stain kit, whereas PE represents the H2AX conjugated antibody.

Annex 3

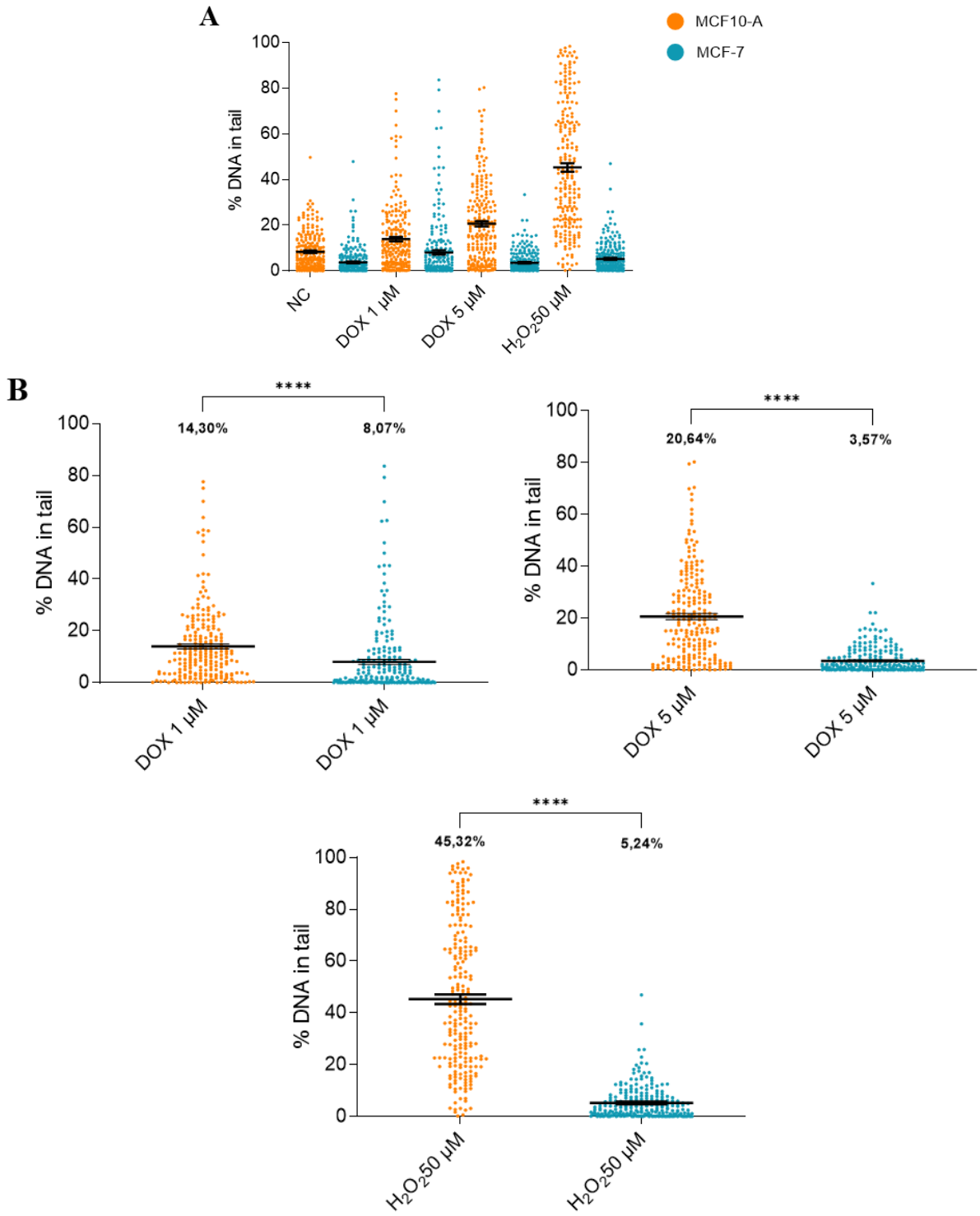

Figure 6.4 - % of DNA in tail in each treatment in MCF10-A versus MCF-7. A- Overall view of different treatments on non-tumorigenic MCF10-A versus tumorigenic cell line MCF-7. B- % of DNA in tail distribution was plotted for each sample and dose using GraphPad Prism 9 software. Mean values ± SEM are represented by the black lines. Statistical analysis with Wilcoxon Matched Pairs test and a p-value < 0.05 was considered statistically significant. Statistical significance is represented with * (the number of * represents how relevant is the statistical difference). All doses presented statistical significance differences, where MCF10-A has a higher % of DNA in tail when compared with MCF-7.

Annex 4

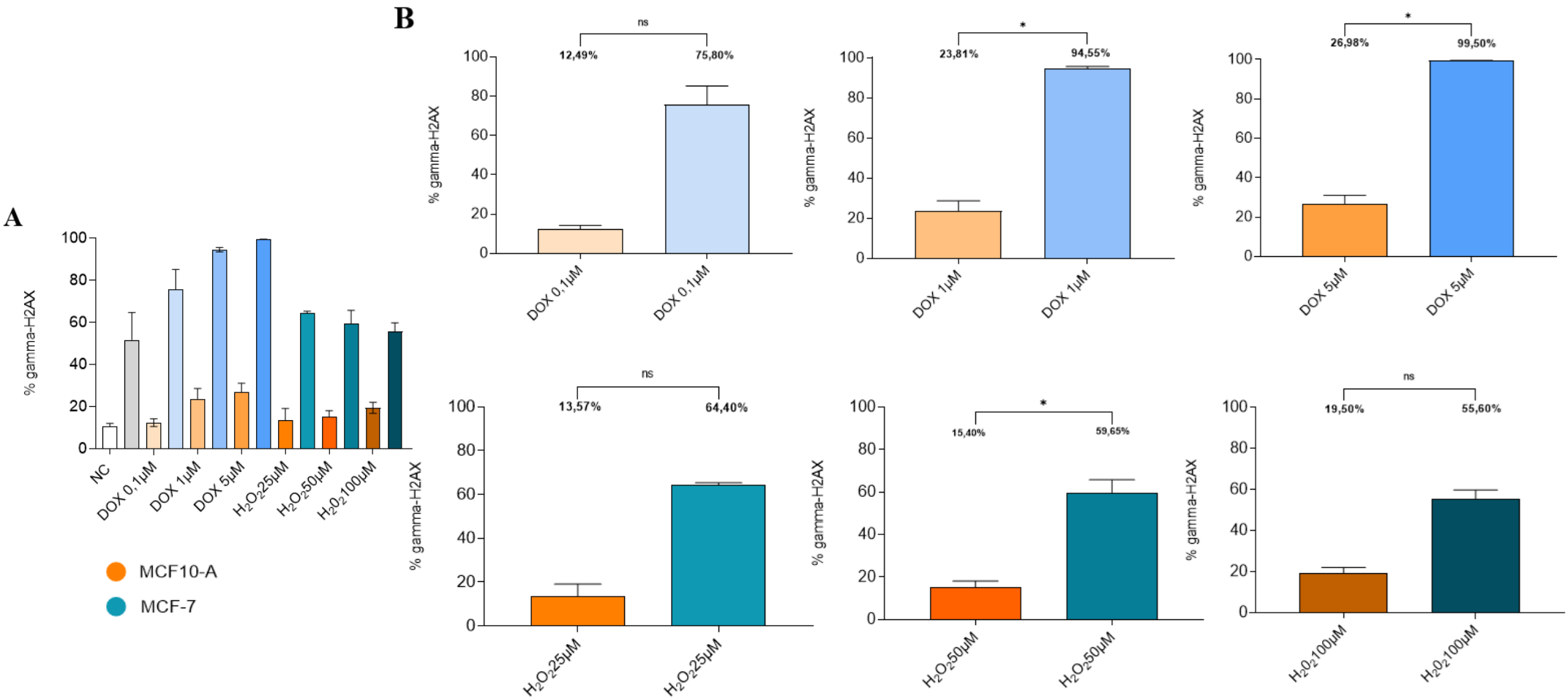

Figure 6.5 – Comparison of % of γ-H2AX in each drug exposure of MCF10-A versus MCF-7. A – Overall % of γ-H2AX in each drug. **B** - % of γ-H2AX in each drug exposure and dose. All graphs were plotted using GraphPad Prism 9 software. Mean values ± SEM are represented by the black lines (orange shades MC10-A and blue shades MCF-7). Statistical analysis with Mann-Whitney test and a p-value < 0.05 was considered statistically significant. DOX 1µM, DOX 5 µM and H_2O_2 50µM presented statistical significance differences, where MCF-7 presents higher % of γ-H2AX. Statistical significance is represented with * (the amount of * represents how relevant is the statistical difference).